Gulf of Mexico Hydrate Mapping and Interpretation Analysis

Phase-II, Project Area 2.2 Report

Aditya Kumar, Alexey Portnov, Ann Cook

February 28, 2023

This report satisfies Mapping and Prospect Identification within Project Area 2.2 for BOEM award Gulf of Mexico Gas Hydrate Mapping and Interpretation Analysis, which is Deliverable/Milestone 3.

Table of Contents

Table 1. List of required deliverables and figures.

Sr.	Deliverable	Figure #
1	A map showing the spatial distribution of BSRs within Project Area 2.2	2
2	RMS amplitude maps showing the possible BSRs in the study area at various depth intervals.	3-10
3	Regional seismic cross sections showing the base of gas hydrate stability and the relationship of prospective reservoir intervals to channel levee systems, faults, salt, and other geologic features.	12-13, 16 -20, 22-27, 31-33
4	Average amplitude maps showing the prospective reservoirs based on direct seismic indicators (peak-leading reflections, phase reversals).	14, 29

1 Study Area and Data

Project Area 2.2 is located in the Green Canyon (GC) protraction area in the northern Gulf of Mexico (Figure 1a). Project Area 2.2 covers an area of ~6300 km^2, with a water depth range between 100 - 1900 m (Figure 1b). A total of 20% of the area has a water depth less than 500 m and is therefore outside of the methane hydrate stability zone (Figure 2).

Thermogenic and biogenic gas hydrates have been recovered in the piston cores at several locations in Project Area 2.2 (Figure 2). The shallowest thermogenic hydrate was recovered at a water depth of 440 m, while the shallowest biogenic hydrate is recovered at 800 m of water depth (Sassen et al., 2001). The morphology of the area is influenced by allochthonous salt, which shapes sedimentary minibasins prone for hydrate accumulations. Salt movement also likely causes slope instability; we observe several submarine landslides in the bathymetry near the mapped BSRs.

The Bureau of Oceans Energy Management (BOEM) previously identified several BSR zones in this area (Shedd et al., 2012) (Figure 2). We describe a total of six BSR systems, two of which were not previously identified by BOEM. The shallowest BSR is observed at a water depth of 900 m in Zone-1 (Figure 2) and occurs on the flank of a salt ridge.

Within Project Area 2.2, we use seven 3D seismic surveys from the National Archive of Marine Seismic Surveys (NAMSS; Triezenberg et al., 2016) database (Figure 1, Table 2), which covers ~ 95% of the total Project Area.

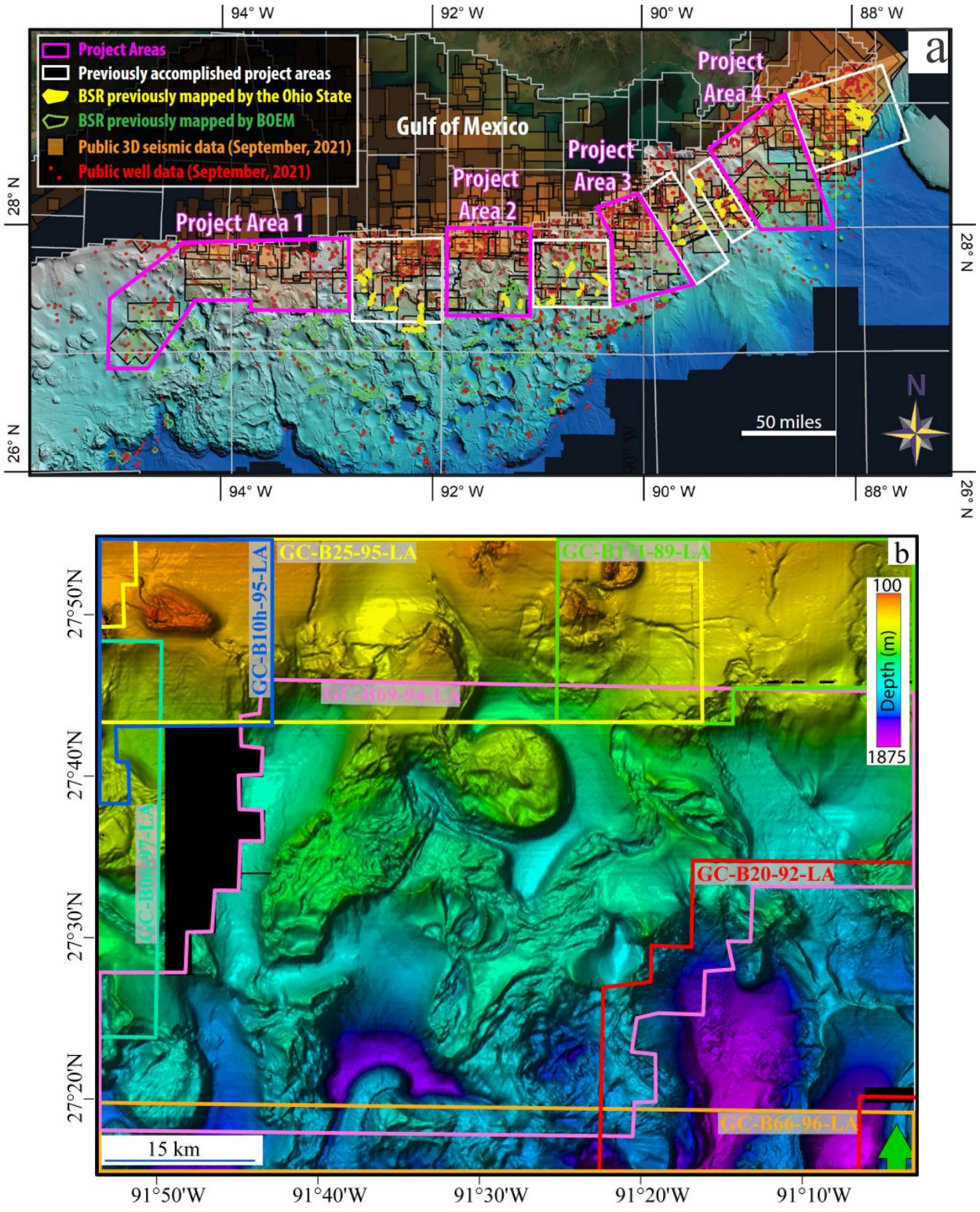

Figure 1: a) A bathymetry map of the northern Gulf of Mexico showing Project Areas of Phase 1 (white squares) and Phase 2 (pink squares). b) Outlines of the seismic surveys used in this study

are rendered over the seafloor bathymetry map of Project Area 2.2. The seafloor bathymetry is mapped in this study using 3D seismic data. The black region shows a 3D seismic data gap.

Survey number	Survey name/BOEM identifier	Year	Area of seismic survey (km^2)	Frequency Range (Hz)	Survey quality	Bin size (m)	Projection
1	B-69-94-LA/L94-069	1994	3200	8-70	Fair	25×12.5	15N NAD 1927, feet
2	B-20-92-LA/L92-020	1992	1000	5-80	Poor	26.6×26.6	15N NAD 1927, feet
3	B-10h-96-LA/L96-10h	1996	425	5-80	Good	12.5×12.5	15N NAD 1927, feet
4	B-25-95-LA/L95-025	1995	1320	5-80	Good	20×12.5	15N NAD 1927, feet
5	B-66-96-LA/L96-066	1996	750	5-85	Good	4×12.5	15N NAD 1927, feet
6	B-06-97-LA/L97-06	1997	300	5-80	Fair	20×12.5	15N NAD 1927, feet
7	B-171-89-LA/L89-171	1989	750	5-80	Fair	25×12.5	15N NAD 1927, feet

Table 2: Details on the 3D seismic surveys uploaded for initial data quality analyses within Project Area 2.2. Projected coordinate systems: NAD_1927_BLM_Zone_15N [EPSG,32066].

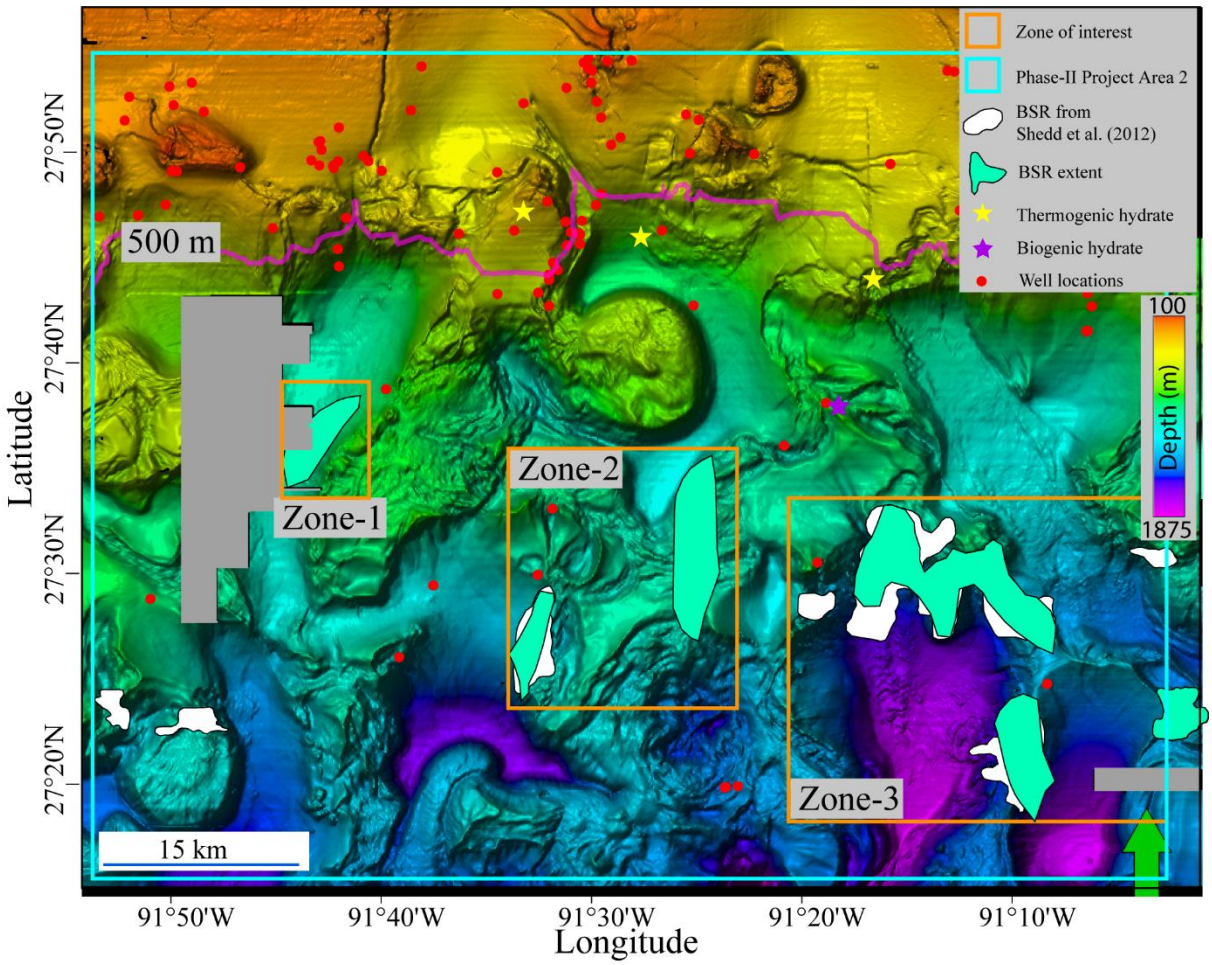

Figure 2: The bathymetry of Project Area 2.2. The white shapes represent the BSRs previously interpreted by BOEM. Light green shapes represent the BSRs interpreted in this report. Interpreted BSRs are grouped into three zones shown by the orange rectangles. The pink line shows the 500 m water depth contour. The gray region shows a gap in public 3D seismic data. Yellow and purple stars show the locations of piston cores where thermogenic and biogenic hydrates were observed Sassen et al., 2001.

2 RMS Mapping

To identify BSR-prone areas in Project Area 2.2, regional root-mean-square (RMS) amplitude calculations were performed independently within all 3D seismic surveys (Figure 1a). The detailed workflow can be found in the report for Phase 1 Project Area 1. The base of the gas hydrate stability zone (GHSZ) is largely a function of water depth and geothermal gradient. Because of multiple heat-conductive shallow salt bodies in this area, the geothermal gradient is highly variable, which significantly perturbs the base of the gas hydrate stability zone. Therefore, RMS amplitude maps are computed within the following depth windows (all in msec below seafloor): 0-50, 50-150, 150-250, 250-350, 350-450, 450-550, 550-650, and 650-750 (Figures 3-10). This allows us to identify BSRs within the wide range of depths where base of the GHSZ can be located and further manually inspect all amplitude anomalies in each seismic volume.

The RMS amplitude investigation led to the identification of BSR systems in three zones (Figure 2, orange rectangles). We determined the extent of each BSR zone using manual, line-by-line interpretation. In Project Area 2.2, BSRs are commonly observed within the depth range of 150-700 msec TWT below the seafloor. The total area spanned by the BSRs in Project Area 2.2 is ~200 km^2.

No paleochannels were identified in Project Area 2.2 utilizing the same method of manual line-by-line interpretation and attribute analyses as used in Project Area 2.4. Possibly, since widespread salt doming began, it significantly limited channelizing over the Project Area 2.2 (Carter et al., 2016). Additionally, modern salt bodies and moderate seismic data quality further complicate the interpretation of the paleochannels in the region.

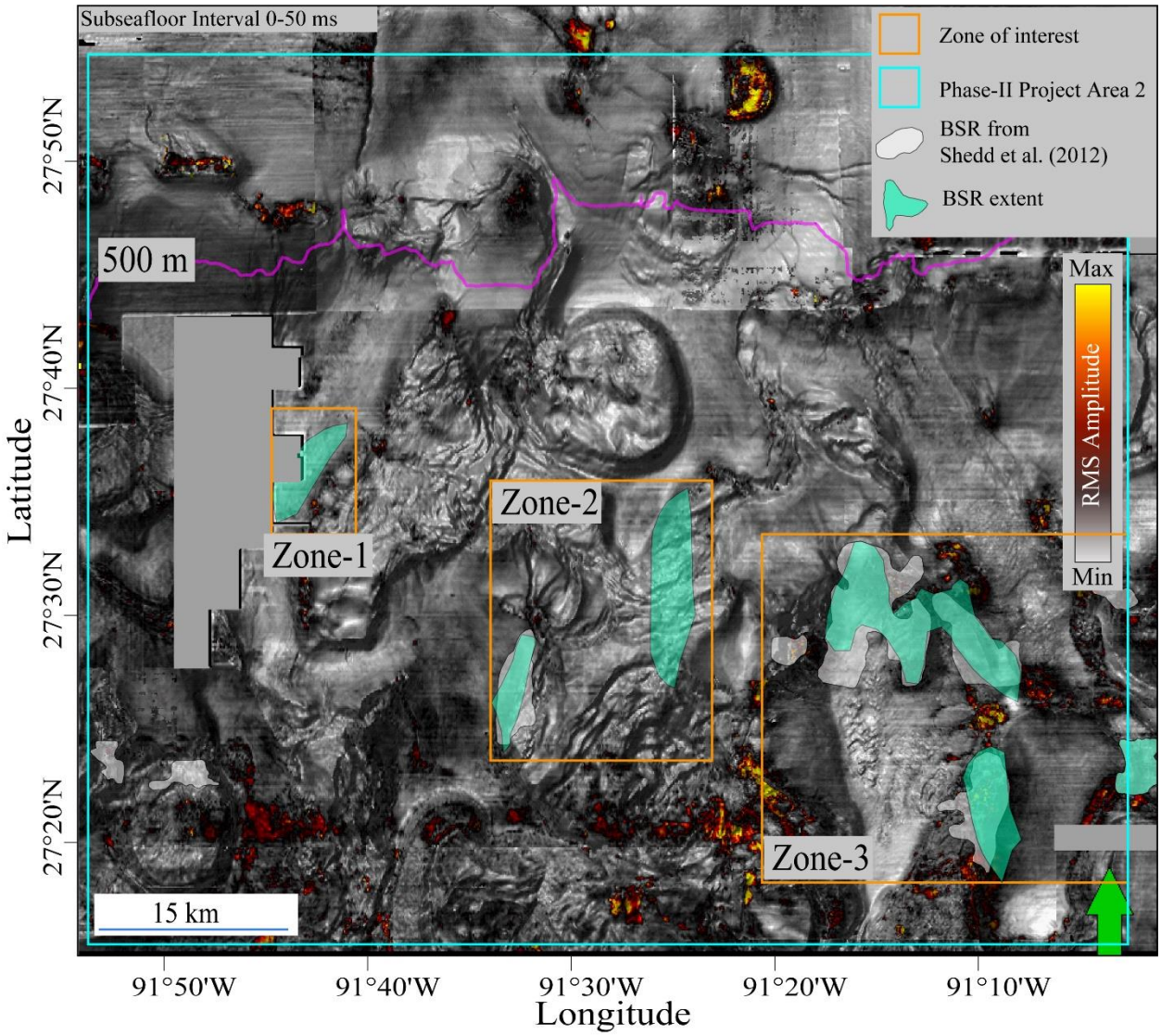

Figure 3: A RMS amplitude map calculated for a subseafloor interval of 0-50 msec. The pink line shows the 500 m water depth contour.

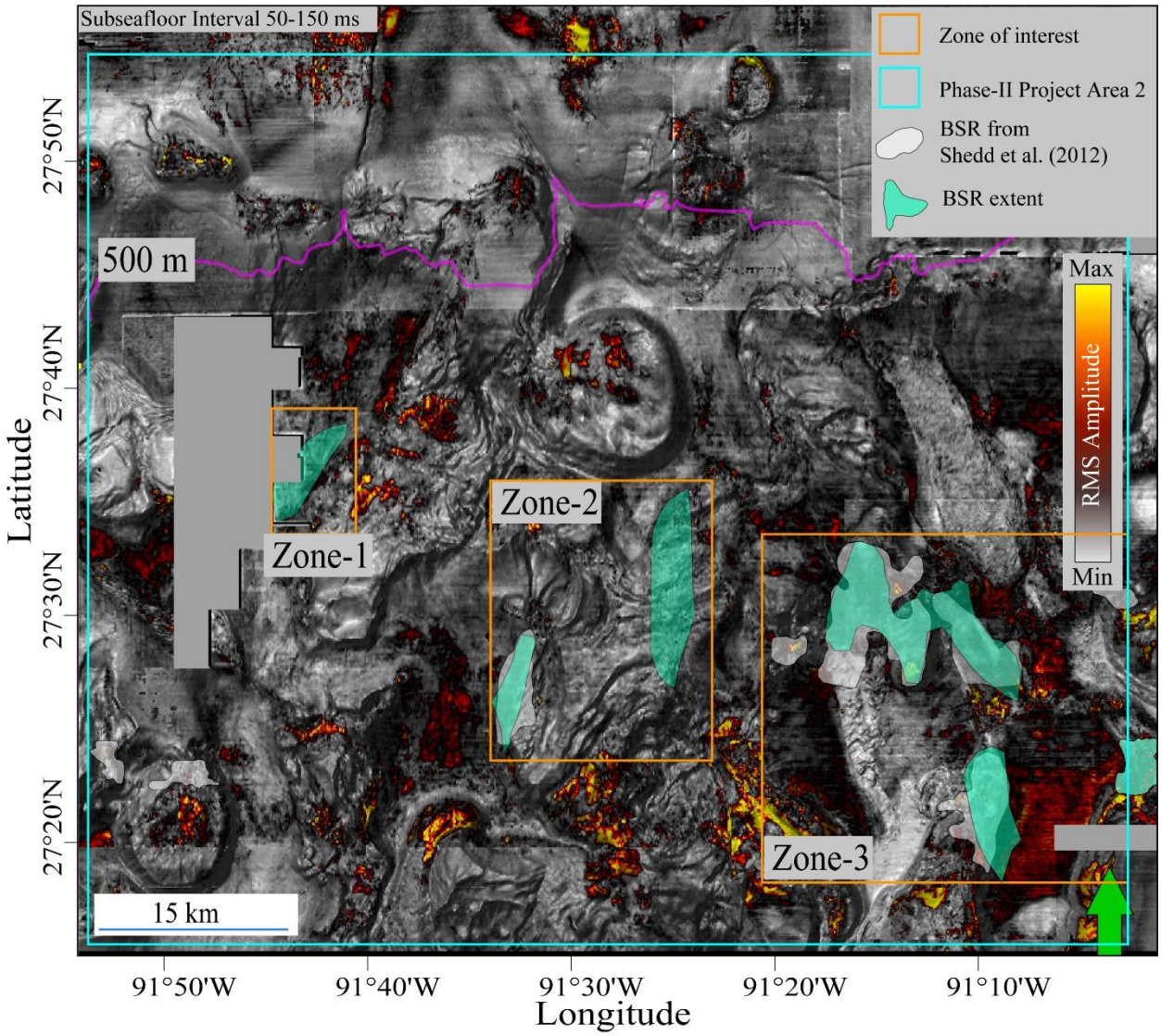

Figure 4: A RMS amplitude map calculated for a subseafloor interval of 50-150 msec. The pink line shows the 500 m water depth contour.

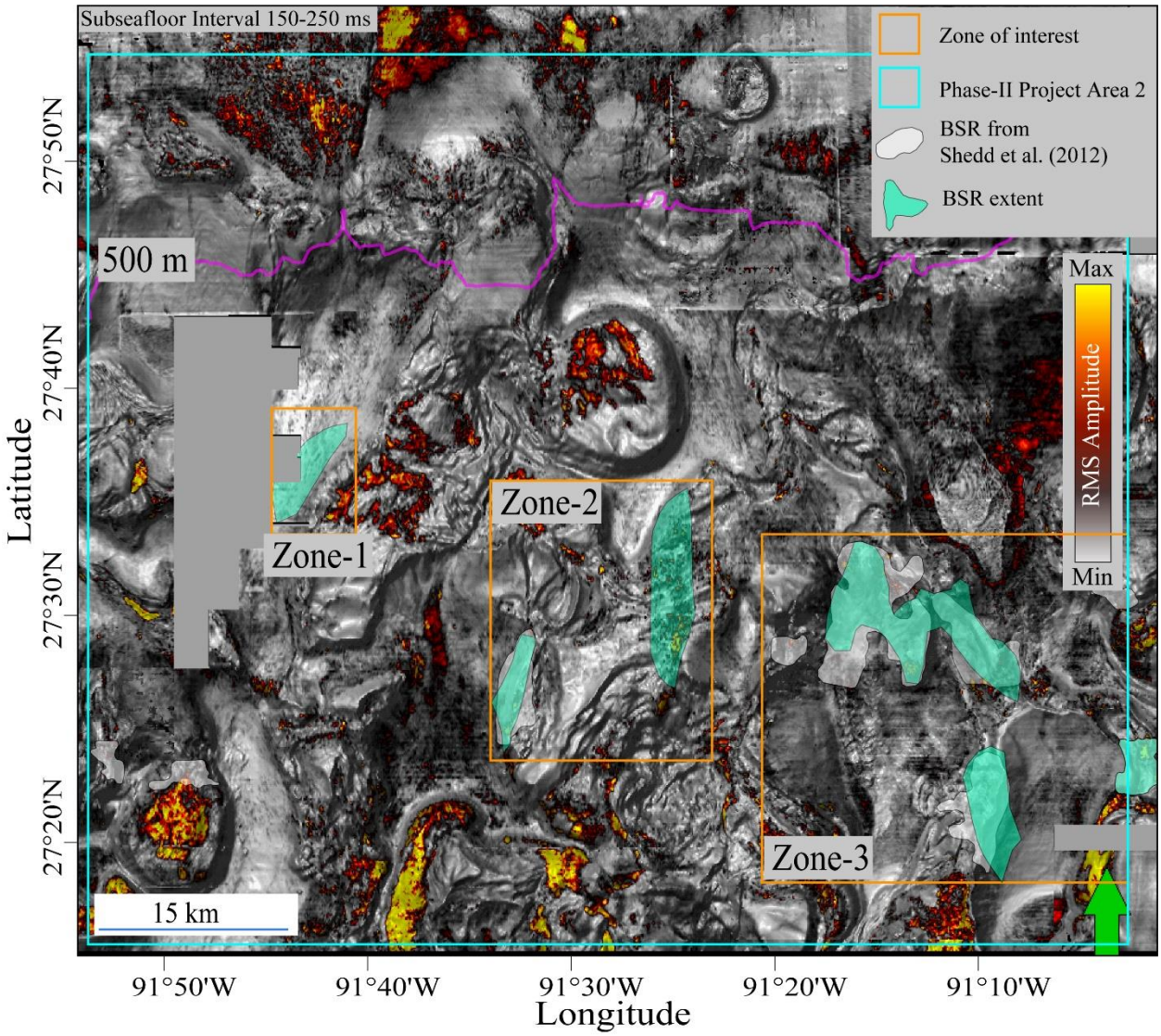

Figure 5: A RMS amplitude map calculated for a subseafloor interval of 150-250 msec. This interval was used to identify the northeastern BSR in Zone-2. The pink line shows the 500 m water depth contour.

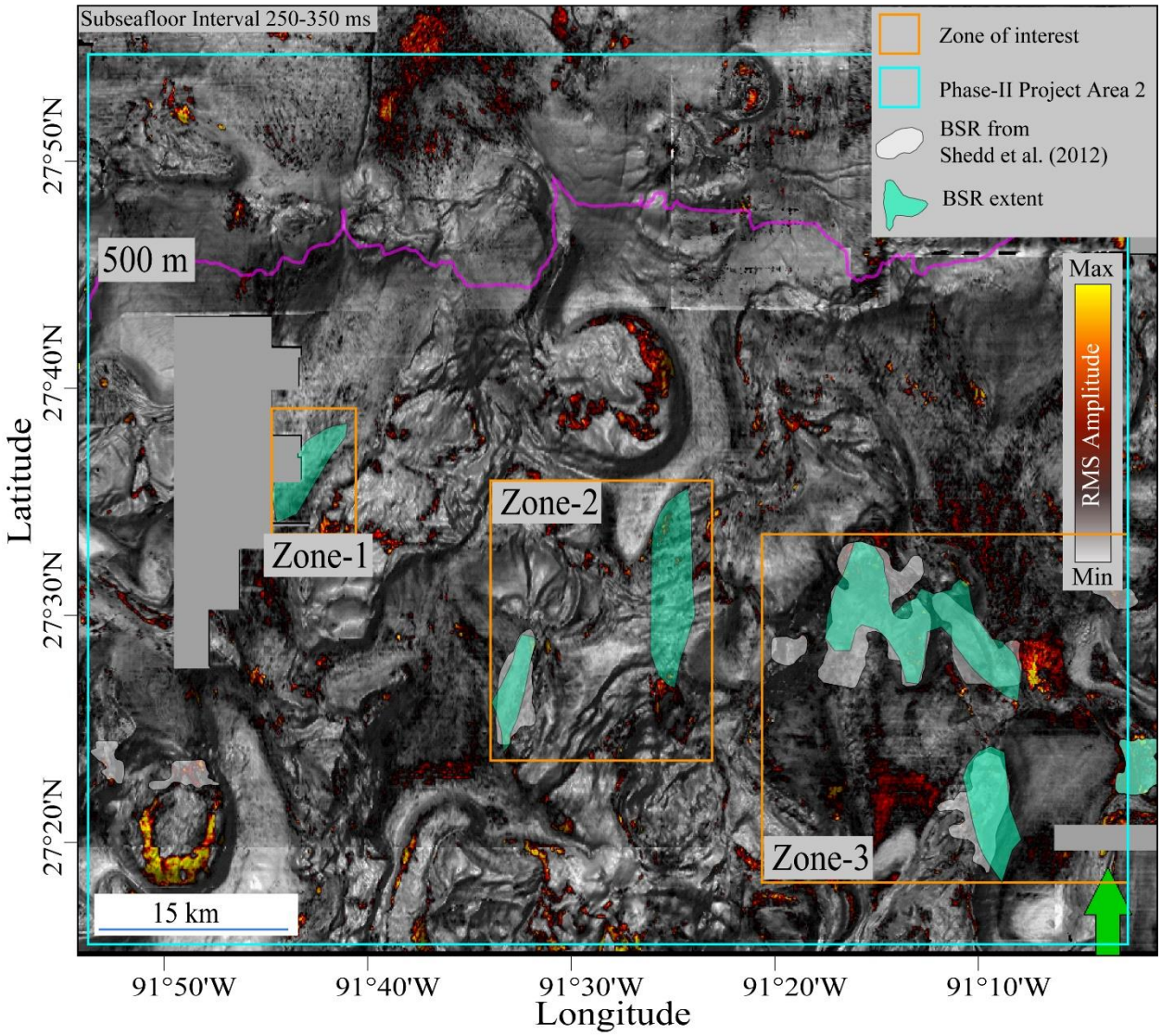

Figure 6: A RMS amplitude map calculated for a subseafloor interval of 250-350 msec. The pink line shows the 500 m water depth contour.

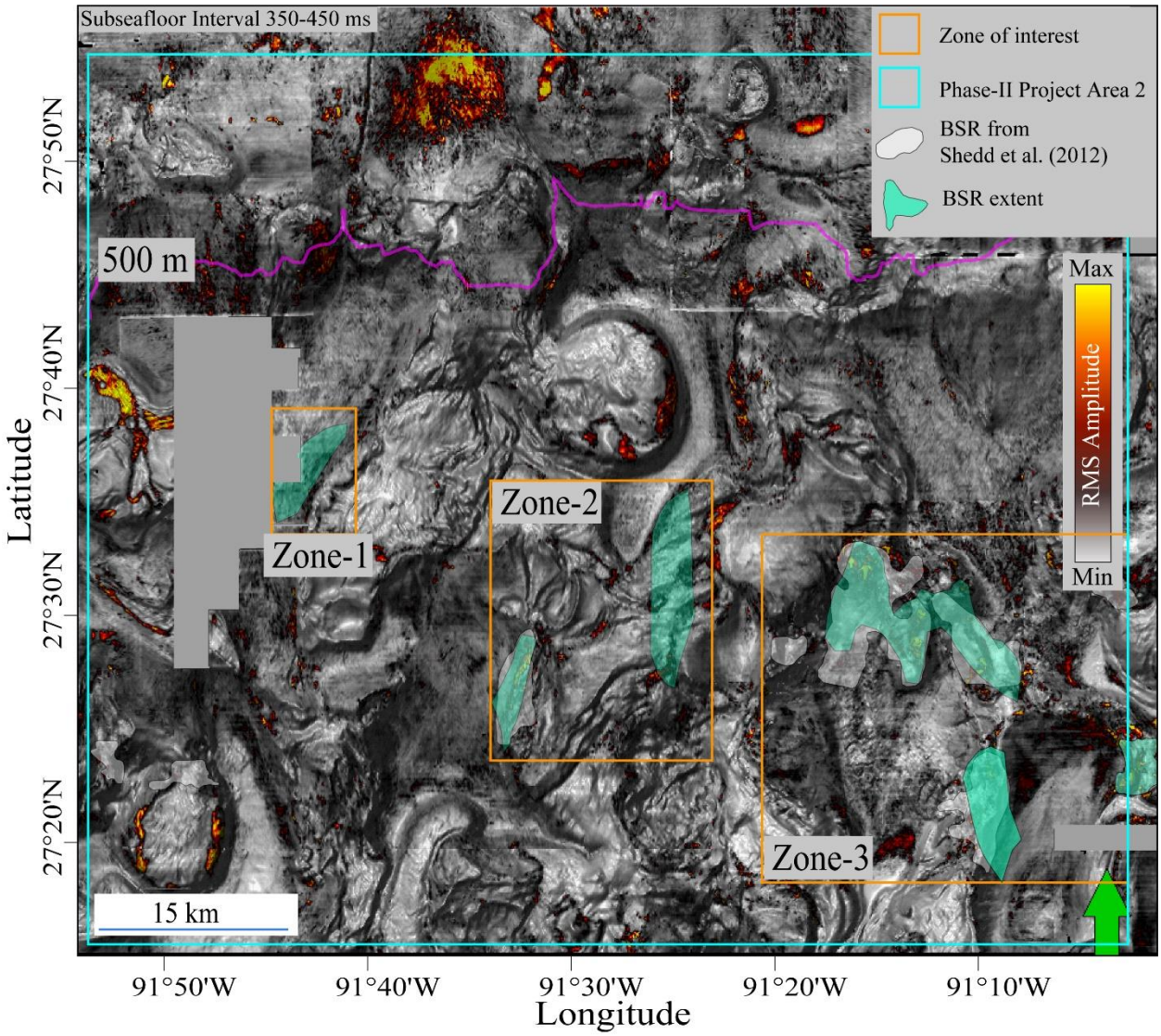

Figure 7: A RMS amplitude map calculated for a subseafloor interval of 350-450 msec. This interval delineates the southwestern BSR in Zone-2. The pink line shows the 500 m water depth contour.

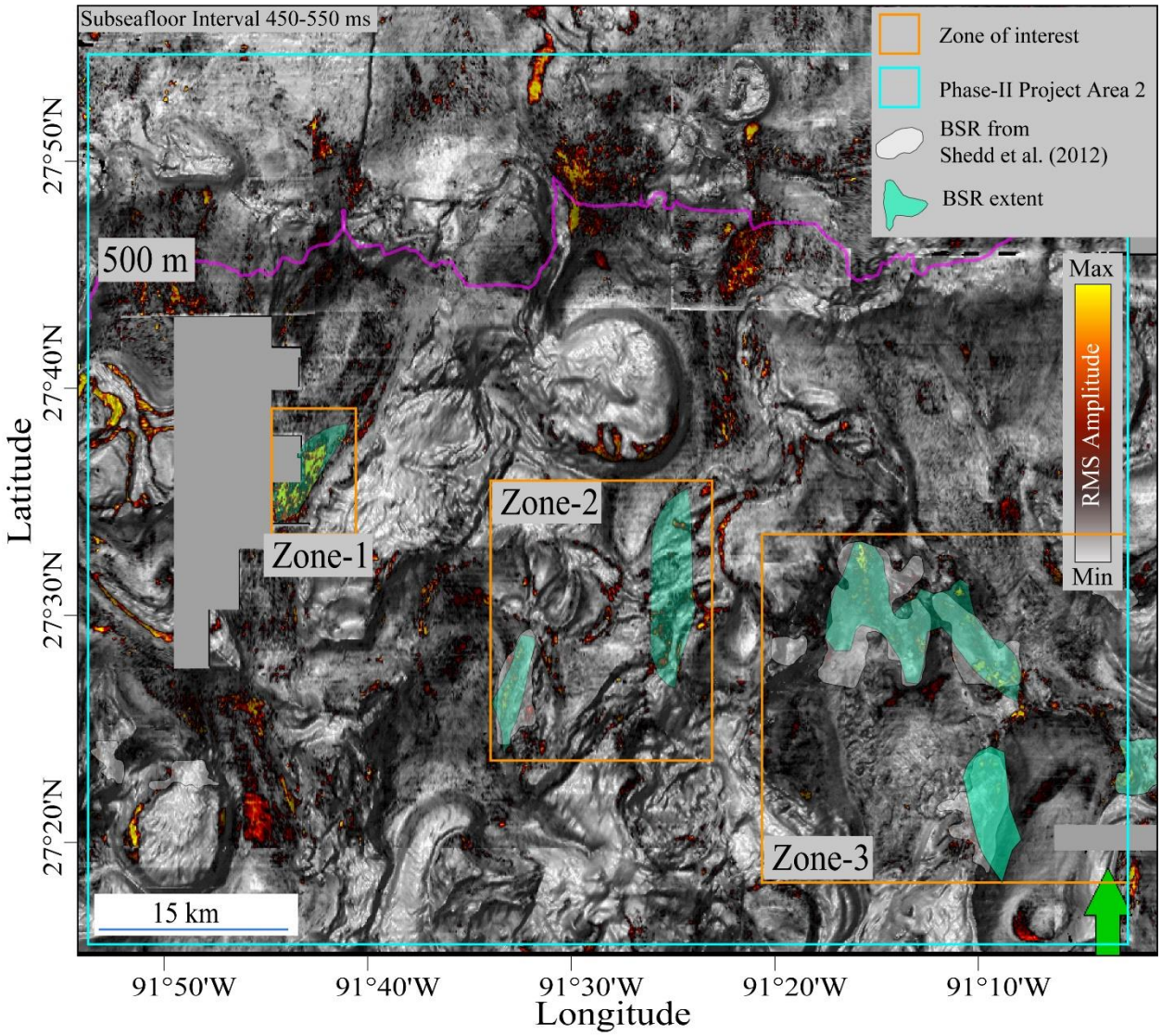

Figure 8: A RMS amplitude map calculated for a subseafloor interval of 450-550 msec. This interval delineates the BSR in Zone-1 and southern and eastern BSR of Zone-3. The pink line shows the 500 m water depth contour.

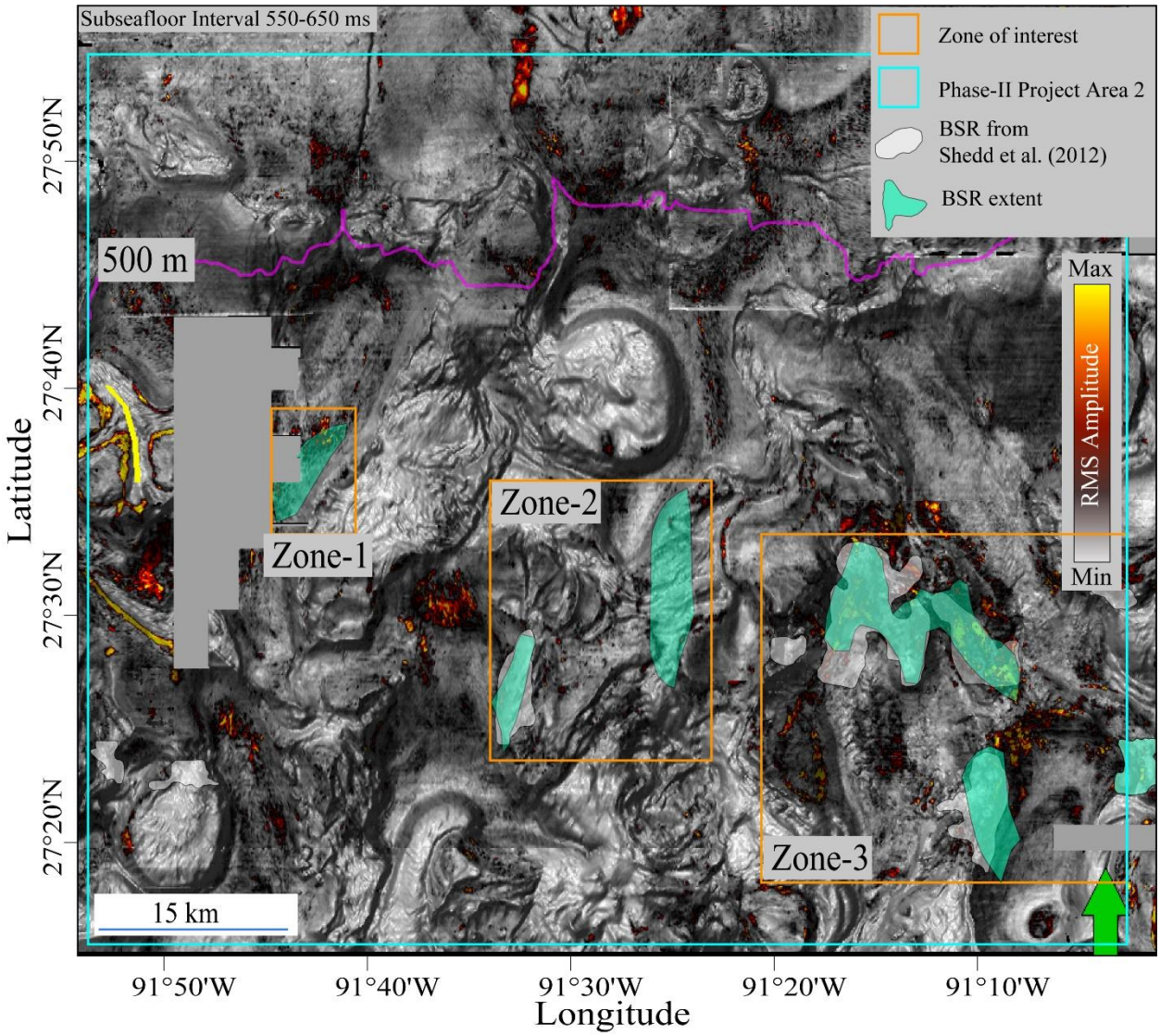

Figure 9: A RMS amplitude map calculated for a subseafloor interval of 550-650 msec. This interval delineates the northern BSRs of Zone-3. The pink line shows the 500 m water depth contour.

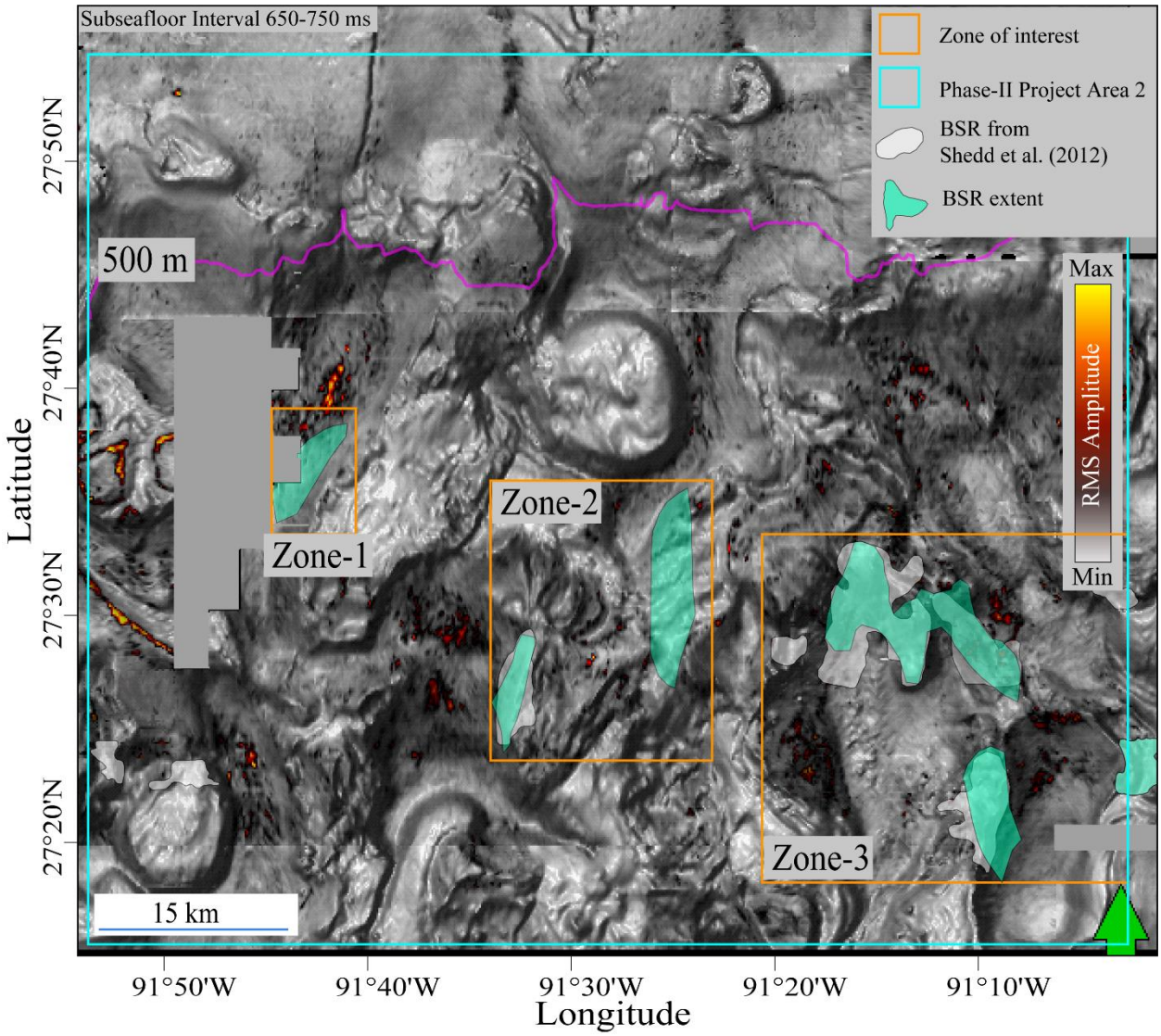

Figure 10: A RMS amplitude map calculated for the 650-750 msec subseafloor interval. The pink line shows the 500 m water depth contour.

3 Classification of BSRs

Herein, we classify the BSRs in three different types based on their characteristics in the seismic data: continuous BSRs, discontinuous BSRs, and clustered BSRs. Continuous BSRs are continuous, coherent seismic reflections with reversed (trough-leading) polarity that crosscuts primary stratigraphy (Hillman et al., 2017; Vanneste et al., 2001). Unlike the continuous BSR, a discontinuous or segmented BSR typically occurs in dipping strata where the BSR at the base of the GHSZ is only recognizable through discreet seismic reflections often coincident with coarser-

grained units. The BSR seismic events are generally parallel to seafloor bathymetry (McConnell and Kendall, 2002; Shedd et al., 2012). A third type of BSR is called a clustered BSR, which is characterized as clustered assemblages of high amplitude reflections roughly aligning with the overlying seafloor bathymetry (Portnov et al., 2019). In particular, clustered BSRs occur in the regions of folding or salt diapir rise because these regions host multiple anticlinal and domal structures that can entrap gas underneath the GHSZ. Such BSRs are common in the Gulf of Mexico and warrant special attention because these BSRs likely indicate high concentrations of gas hydrate in turbidite sands (Portnov et al., 2019).

4 Results in Project Area 2.2

4.1 Zone -1

Zone-1 is located in the western part of Project Area 2.2 (Figure 2). Water depth in this zone varies between 750-1000 m. We identify one new BSR system in this zone that was previously unidentified by BOEM. This system spans an area of ~20 km^2 and is present at the flank of a salt ridge (Figure 11a, 12 and 13). This BSR is present at 450-500 msec TWT below the seafloor (Figure 12, 13), or approximately 380-420 meters below the seafloor (mbsf) using 1700 m/s average sediment velocity. An RMS amplitude map calculated within 450-550 msec window below the seafloor shows the spatial extent of the BSR system (Figure 11b). BSRs in this system show various acoustic characteristics: continuous, discontinuous and clustered (Figures 12, 13). Above the clustered BSR, we observe a patch of peak leading reflections (Figure 12). This peak-leading reflection spans a small area of ~ 1 km^2 (Figure 14) and potentially contains high saturation gas hydrate. In Figure 14, there are several high amplitude patches but only one high confidence patch is marked.

Well API #608114049800 is the nearest to this BSR system, located ~2km away (Figure 2). The stratigraphic layers observed within and above the BSR zone are roughly mapped up to the well location (Figure 15b). Well log data that maps to the sediments in our zone of interest occurs from ~3100-4200 ft in the well. There are slight increases in resistivity above background (~1 Ωm) but the overall measured resistivity is very low (all less than 2 Ωm), so it is difficult to determine if these increases are related to gas, gas hydrate, changes in porosity or changes in lithology. At most,

there may be low saturations of hydrate or gas in the well (Figure 15C). From 3200-3900 ft, we observe the primary lithology is marine mud. From ~3900-4150 ft we observe an interval with interbedded sand-rich layers; this interval maps to the approximate depth of and below the BSR in Zone 1 (Figure 15B), suggesting this interval may be sand prone.

We derive geothermal gradients from the BSR assuming an equilibrium model: 1) heat flow is constant, one-dimensional (vertical) and occurs only through conduction; 2) pore pressure is hydrostatic; 3) pore fluid salinity is 3.5 %; and 4) gas composition is pure methane. We estimate the geothermal gradient in Zone-1 between 20°- 25° C/km (Table 3).

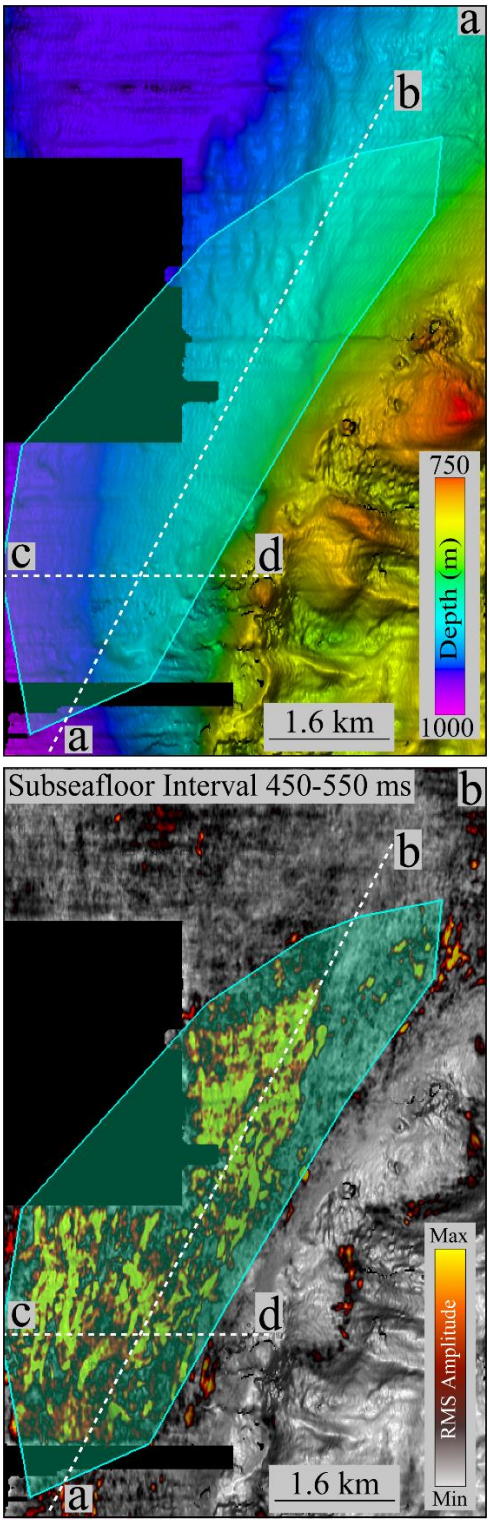

Figure 11: a) A bathymetry map showing a BSR extent within Zone-1 of Project Area 2.2. b) A RMS amplitude map of the sub-seafloor interval between 450-550 msec.

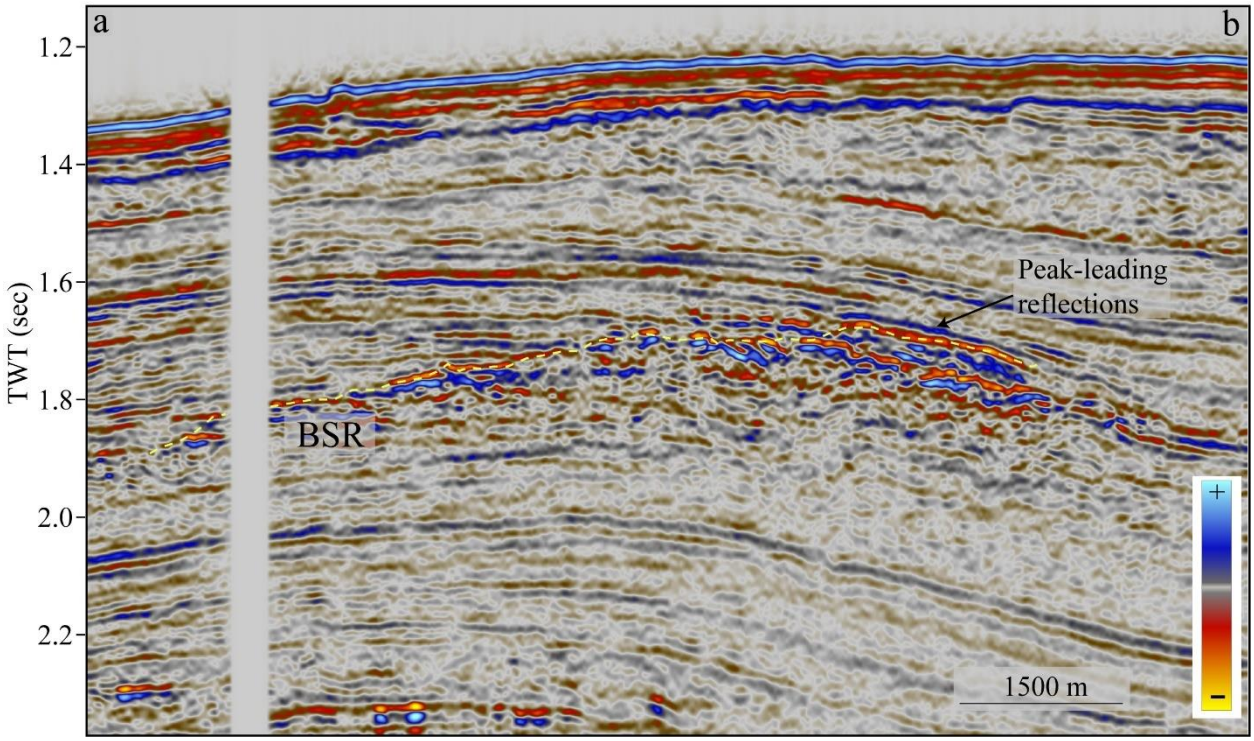

Figure 12: A seismic profile showing a south-north cross-section across the BSR system of Zone-1. The profile location is shown in Figure 11.

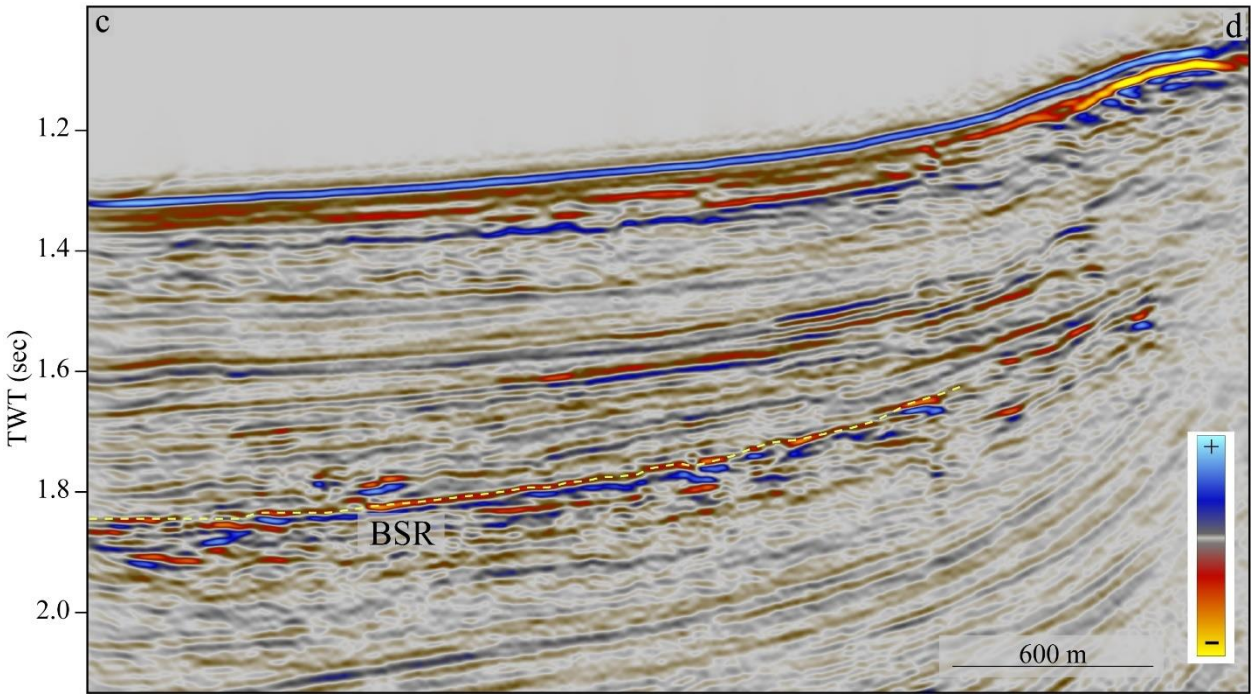

Figure 13: A seismic profile showing a south-north cross-section across the BSR system of Zone-1. The profile location is shown in Figure 11.

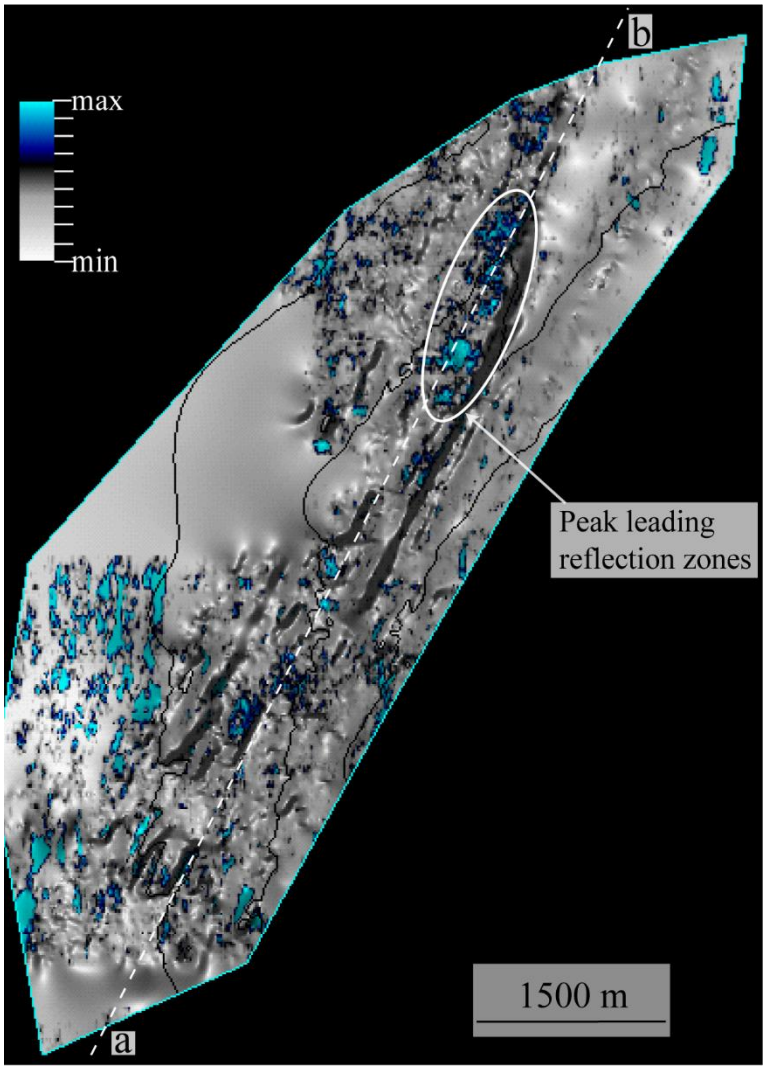

Figure 14: A map of average positive amplitude calculated within a 30 msec window above the BSRs in Zone-1. Peak leading reflection zones are circled with the white ellipse.

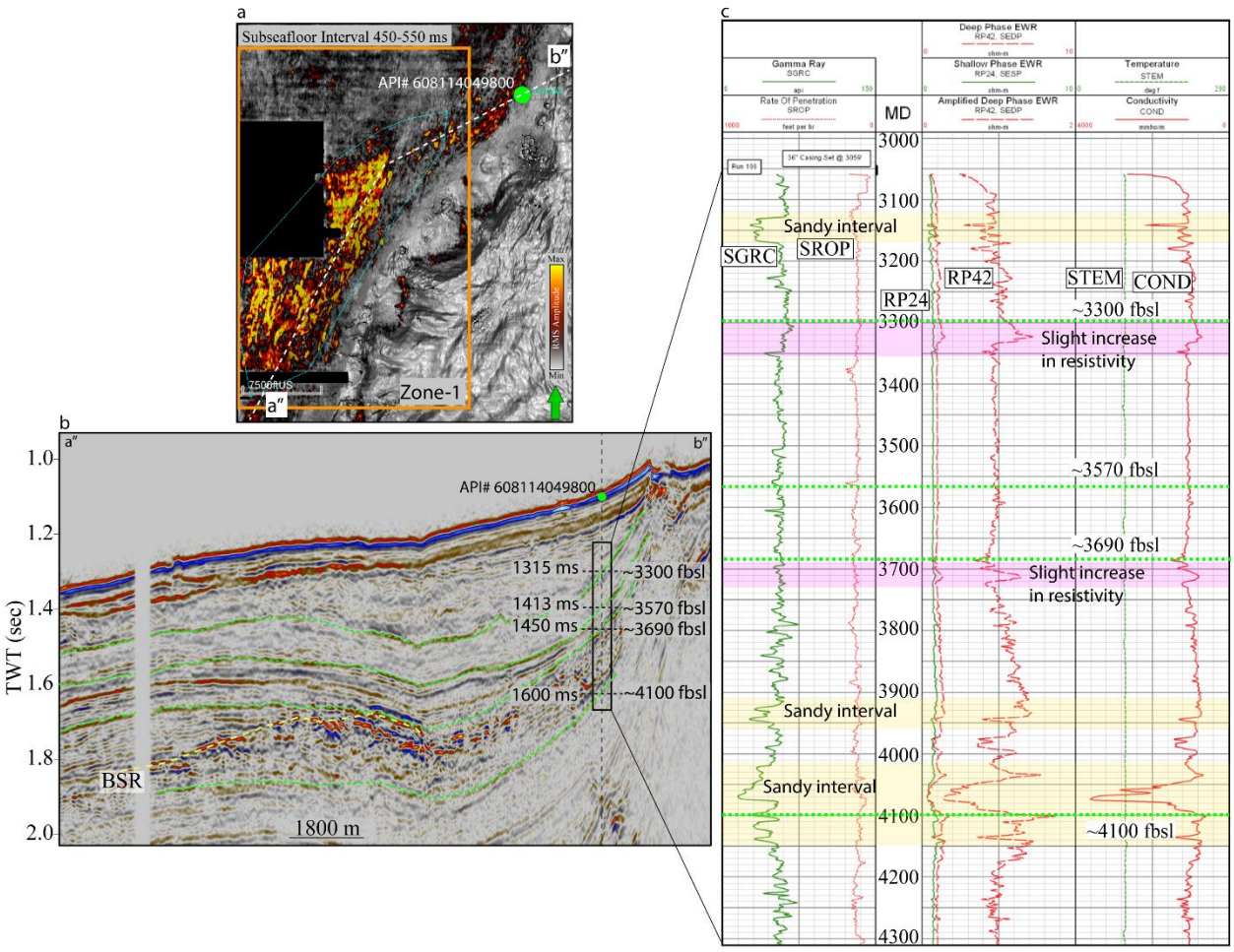

Figure 15: a) The RMS amplitude map of Zone-1 within the subsurface interval of 450-550 ms. The green circle shows the location of well with API# 608114049800 and the white dotted line indicates the location of the seismic profile shown in b). c) The well logs in API# 608114049800.

Zone	Seafloor TWT (msec)	BSR TWT (msec)	Seafloor Depth (m)	BSR depth below seafloor (m)	BSR depth from sea surface (m)	Geothermal Gradient (°C/km)
1	1000 - 1350	1600 - 1850	750 -1000	380 - 420	1130 -1420	20 - 25
2	1100 - 1700	1400 - 2150	850 - 1300	125 - 450	975 -1750	30 - 60
3	1100 - 2500	1500 - 2800	850 - 1900	200 - 600	1050 - 2500	25 -53

Table 3: The seafloor depth, BSRs depth and geothermal gradient in the identified zones.

4.2 Zone-2

Zone-2 is located in the central part of Project Area 2.2 (Figure 2). We identify two BSR systems in this zone in water depths of 850-1300 m (Figure 16). Both systems are mapped using the 3D seismic volume B-69-94-LA. The BSRs in both systems are discontinuous and associated with salt ridges (Figures 16-20). The southwestern system was previously identified by BOEM and also confirmed in this study (Figure 16). The BSR in the eastern part of Zone-2 was not previously identified by BOEM.

The eastern BSR is present above a salt ridge and spans a 44 km^2 area (Figure 16). This BSR depth varies between 150–220 msec TWT (~125–190 m) below the seafloor. A RMS amplitude map calculated for a depth of 150-350 msec TWT below the seafloor shows the extent of the BSR (Figure 16b). Seismic profiles across this system are shown in Figures 17 and 18. In both profiles, we observe a discontinuous BSR present within a possible structural trap caused by shallowing of the salt.

The southwestern BSR system is smaller and spans a 14 km^2 area. BSRs are present over the salt ridge and extend towards the minibasin (Figures 16, 19, and 20). BSRs in this system are identified at 200-450 ms TWT (~170 – 380 m) below the seafloor. BSRs are shallower above the salt ridge and deepen away from the ridge. We do not see any paleochannel signatures in this region or near the BSRs.

The geothermal gradient in the eastern system in Zone-2 is ~50-60°C/km. The geothermal gradient in the southwestern system of Zone-2 is higher (~ 60°C/km) above the salt and gradually drops down to ~30°C/km towards minibasin.

The closest well to the SW BSR is 1.5 km away but does not provide any information that could inform the lithological analysis of the shallow system.

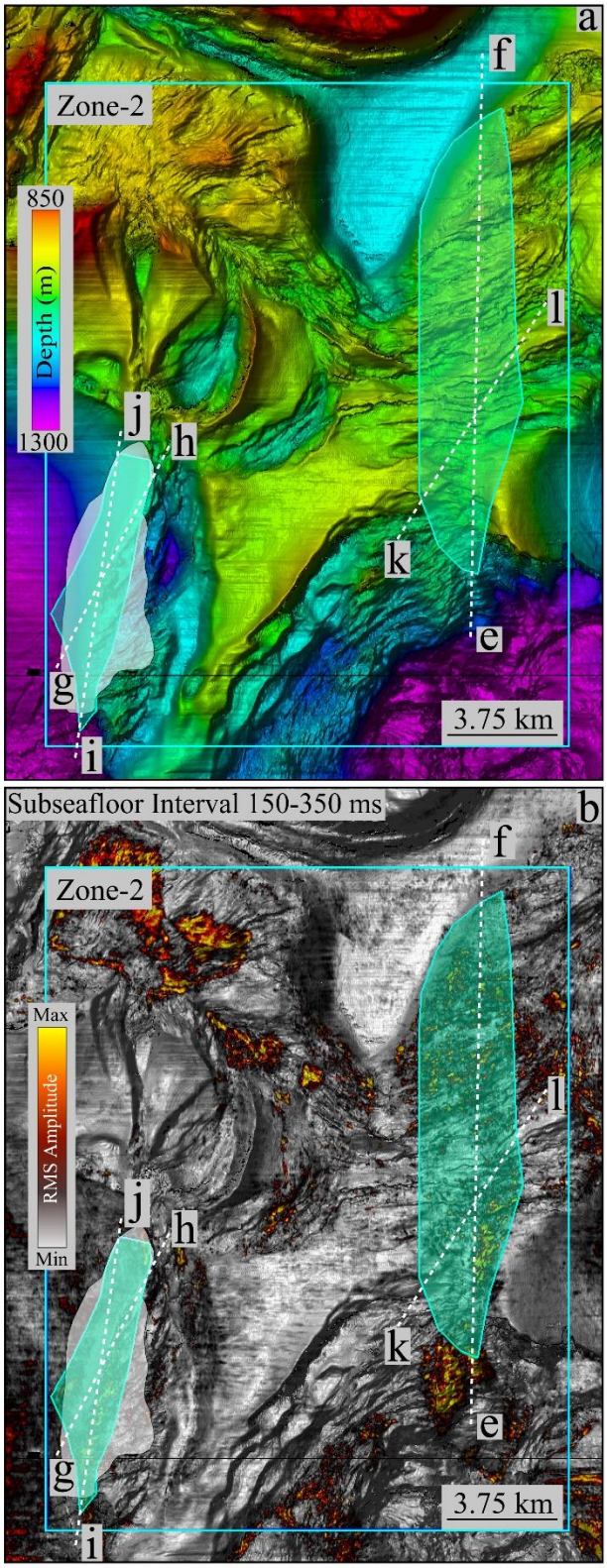

Figure 16: a) A bathymetry map showing the BSR extent within Zone-2 of Project Area 2.2. b) A RMS amplitude map of the sub-seafloor interval between 150-350 msec.

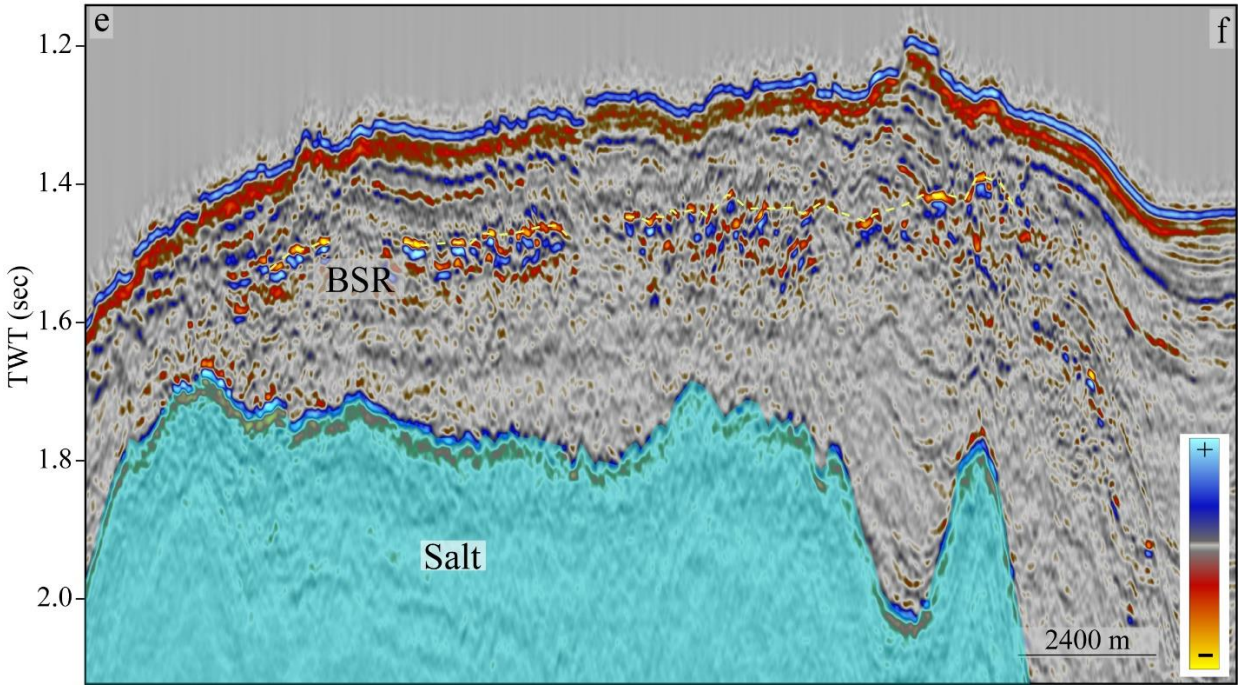

Figure 17: A seismic profile showing a south-north cross-section across the eastern BSR system of Zone-2. A discontinuous BSR is observed above the salt as shown by the yellow dashed line. The profile location is shown in Figure 16.

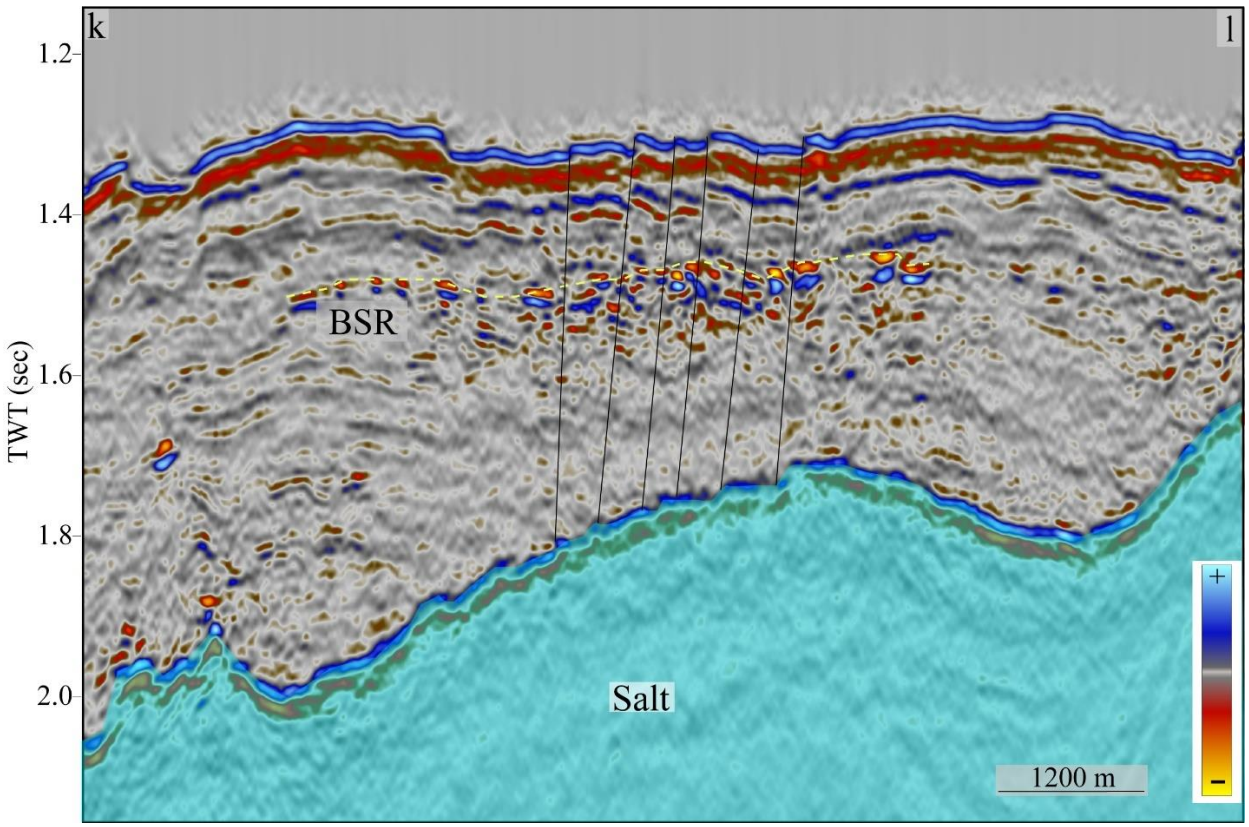

Figure 18: A seismic profile showing a southwest-northeast cross-section across the eastern BSR system of Zone-2. A discontinuous BSR is observed above the salt as shown by the yellow dashed line. The profile location is shown in Figure 16.

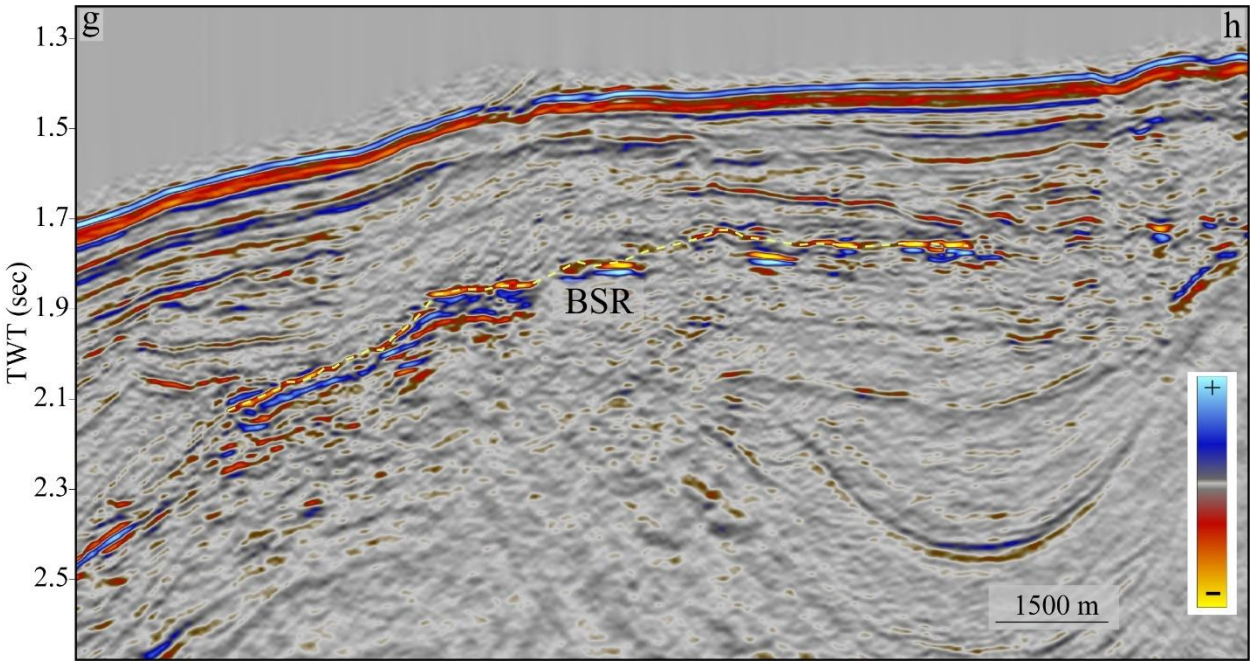

Figure 19: A seismic profile showing a southwest-northeast cross-section across the southwestern BSR system of Zone-2. A discontinuous BSR is marked with yellow dashed line. The profile location is shown in Figure 16.

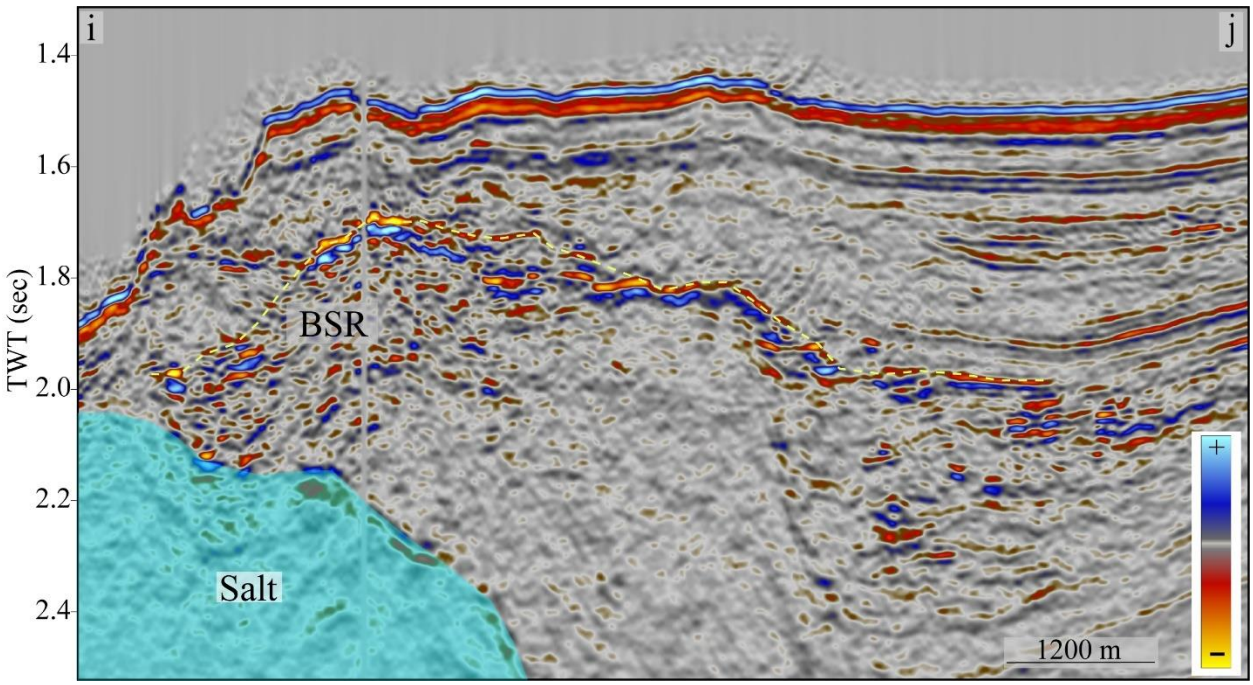

Figure 20: A seismic profile showing a south-north cross-section across the southwestern BSR system of Zone-2. A discontinuous BSR is marked with yellow dashed line. The profile location is shown in Figure 16.

4.3 Zone -3

Zone-3 is located in the southeastern part of the Project Area 2.2 (Figure 2). The water depth in this area ranges between 850-1900 m (Figure 21). We map three BSRs in this area which were previously identified by BOEM. All systems are mapped using 3D seismic volume B-20-92-LA. BSRs in the north, south, and east span an area of 80 km^2, 30 km^2, and 15 km^2, respectively. All three BSR systems are associated with salt structures and are discontinuous (Figure 21-26, 31-33).

The northern BSR system in Zone-3 is the largest BSR system in Project Area 2.2. The BSR depth varies between 300-600 msec TWT (~250-500 m) below the seafloor. Near salt, we observe several landslide features in seafloor bathymetry and seismic sections. Figures 22-24 show the seismic cross-sections across this northern BSR. All seismic sections show a clear discontinuous BSR. The south-north profile at the center of this BSR (Figure 24) may indicate presence of a double BSR. Figure 21 shows the extent of this double BSR that spans an area of ~1.5 km^2. The second BSR might be formed due to the presence of thermogenic hydrate. Since gas

chromatograph data is not collected near these features, it is difficult to understand the cause of the double BSRs at this location.

The southern BSR system is also associated with a salt structure and extends towards the minibasin to the east (Figure 21). The BSR depth of the southern BSR system varies between 400-700 msec TWT (~340-600 m) below the seafloor. Figures 25-27 show the seismic profiles across this system. Above the salt, the BSR is shallower and deepens toward the minibasin. We observe a possible seismic phase reversal just above the BSR (Figure 25-28). We manually track this phase reversal and it spans an area of ~ 2.5 km^2 and show the instantaneous amplitude along the phase reversal horizon in Figure 29. The updip edge of the phase reversal horizon is associated with a fault as shown in Figure 28. The downdip edge of the phase reversal horizon may be associated with a fault, but this fault, if present, is hard to define due to poor seismic data quality. The downdip gas leg is present between 1950-2200 mbsl. Based on the dominant frequency of the seismic signal, the thickness of the hydrate horizon is roughly around 13-15 m. The nearest well (API# 608114022900) is ~ 2 km away from the interpreted BSR (Figure 2, 30a). A seismic profile across the BSR zone and the well is shown in Figure 30b. The well log data that maps to the zone of interest occur from ~4500 – 6900 ft (Figure 30b). The resistivity at some intervals in the well increases slightly above background (~1 Ωm) but remains less than 2 Ωm (Figure 30 b,c). Because these variations are not significant, it is difficult to determine whether these variations are related to gas, gas hydrate, or change in lithology and/or porosity. We observe a low gamma and low resistivities in the well at a depth of ~6400 (Figure 30c); this interval maps to the approximate depth of BSR (Figure 30b), suggesting this may be a sand-rich interval.

The BSR in the east is located at 230-500 msec TWT (~200-425 m) below the seafloor. Figures 31-33 show the seismic cross-sections across this system. An underlying salt body below the eastern BSR causes faulting in the shallow sediments (Figures 31 and 32). These faults might be responsible for the fluid flow towards the hydrate stability zone and the hydrate accumulation. Several seafloor landslide features are also observed in the area of the eastern BSR.

The estimated geothermal gradient in the northern system in Zone-3 is ~25°-45° C/km. The geothermal gradient in the southern system of Zone-3 is ~25°-40° C/km. In the eastern BSR system, the geothermal gradient varies between ~35°-53° C/km. High geothermal gradient is attributed to the increased heat flow associated with the conductivity of shallow salt in this region.

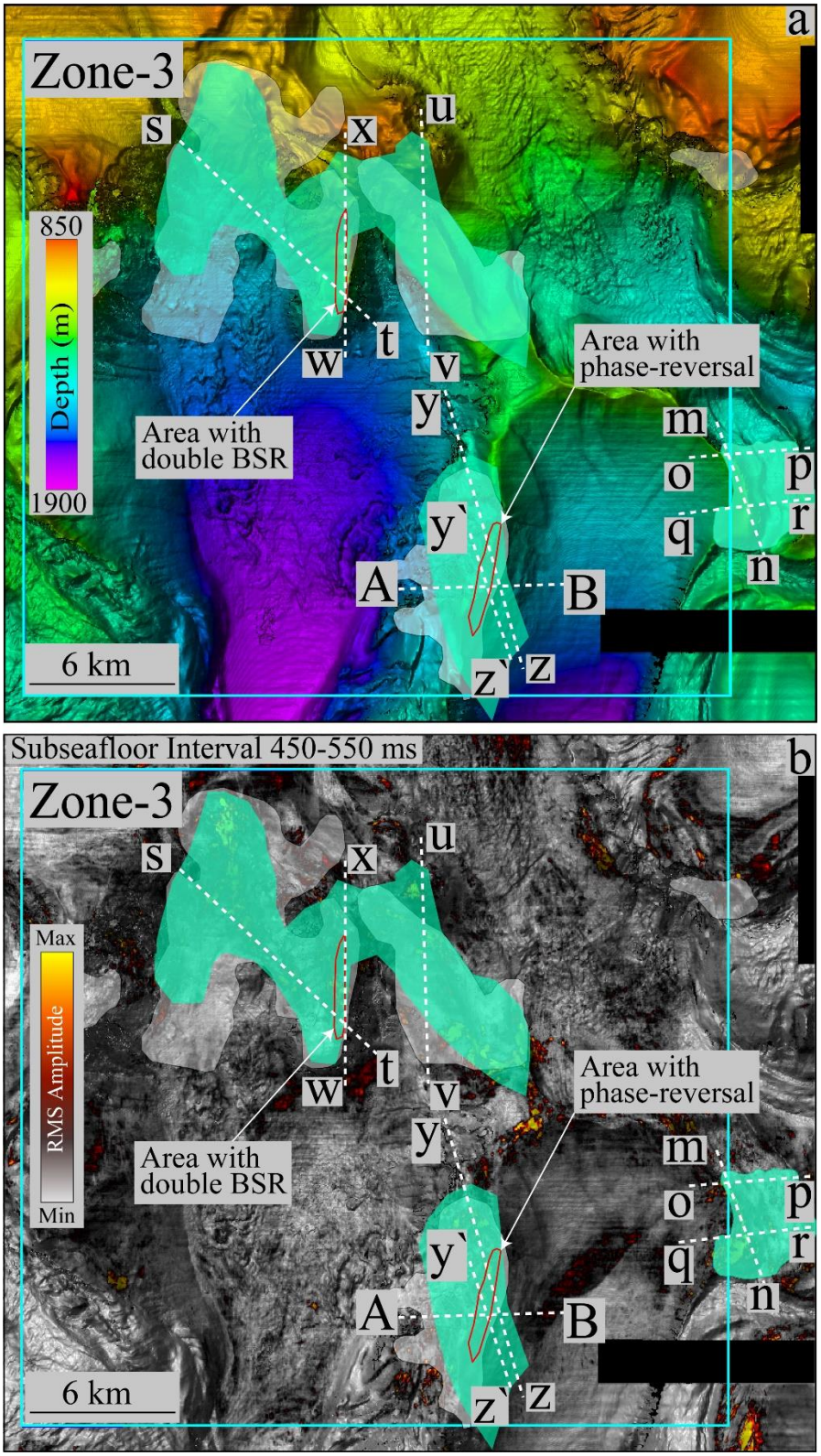

Figure 21: a) A bathymetry map showing the BSR extent within Zone-3 of Project Area 2.2. b) A RMS amplitude map of the sub-seafloor interval between 450-600 msec.

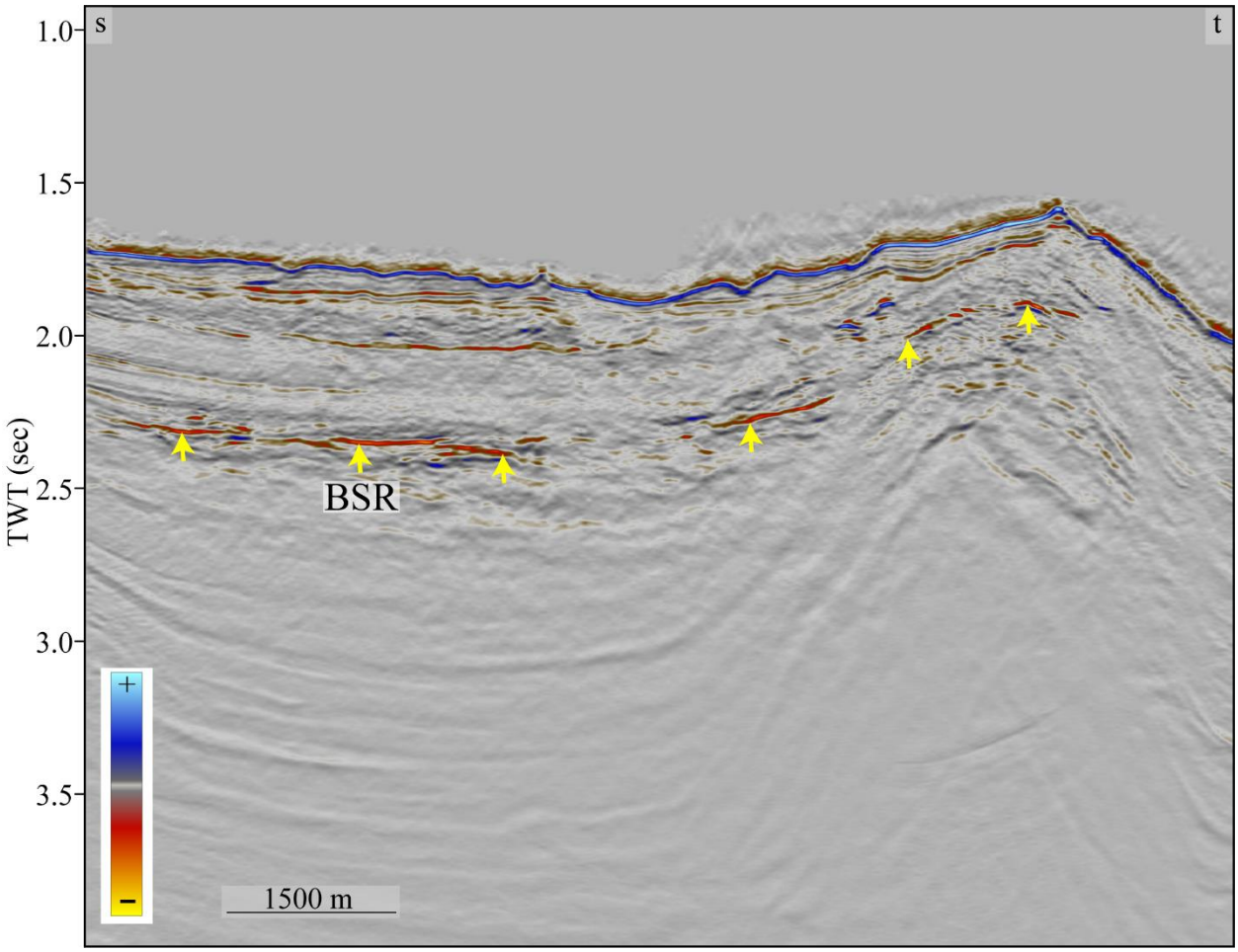

Figure 22: A seismic profile showing a northwest-southeast cross-section across the northern BSR system of Zone-3. A discontinuous BSR is marked with yellow arrows. The profile location is shown in Figure 21.

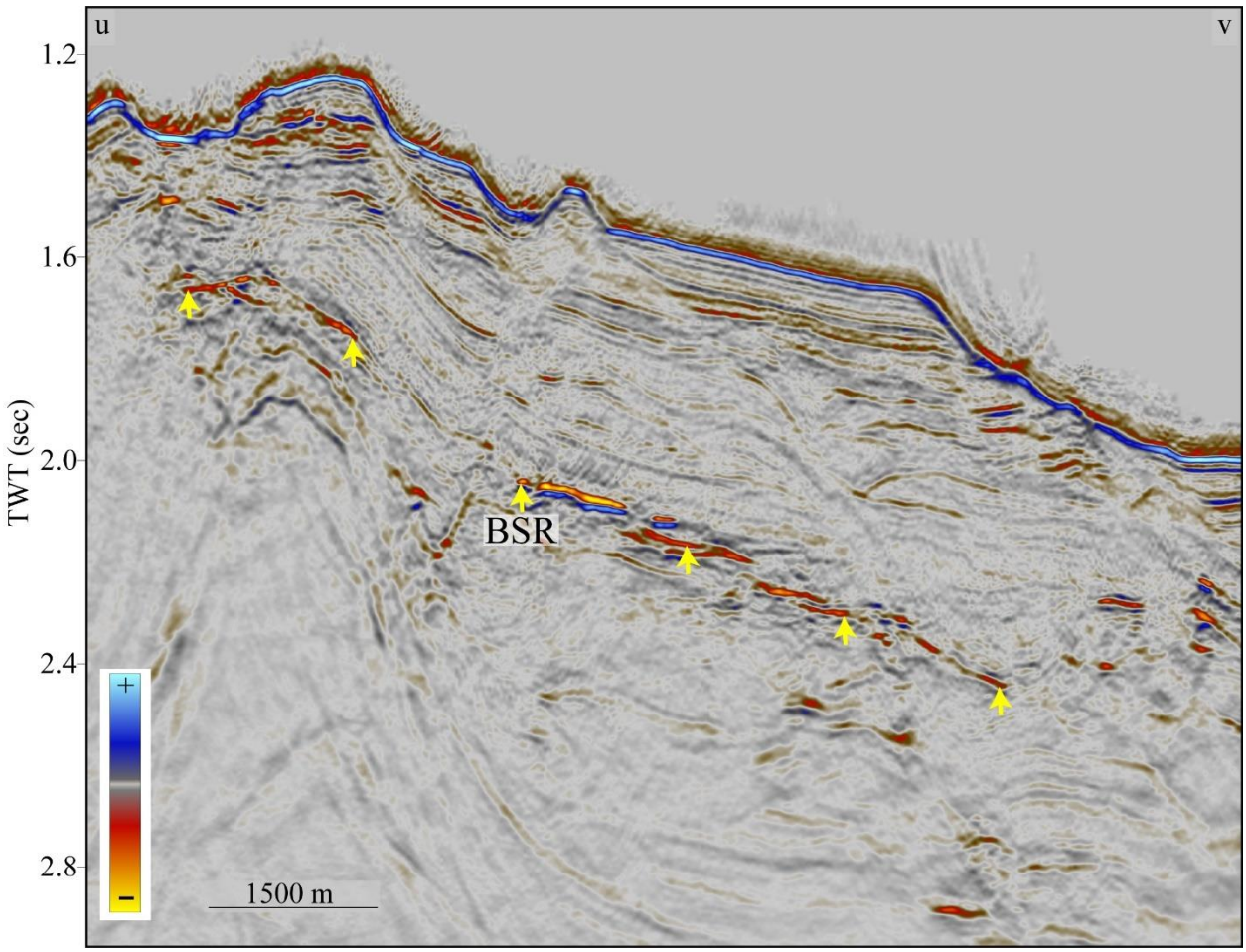

Figure 23: A seismic profile showing a north-south cross-section across the northern BSR system of Zone-3. A discontinuous BSR is marked with yellow arrows. The profile location is shown in Figure 21.

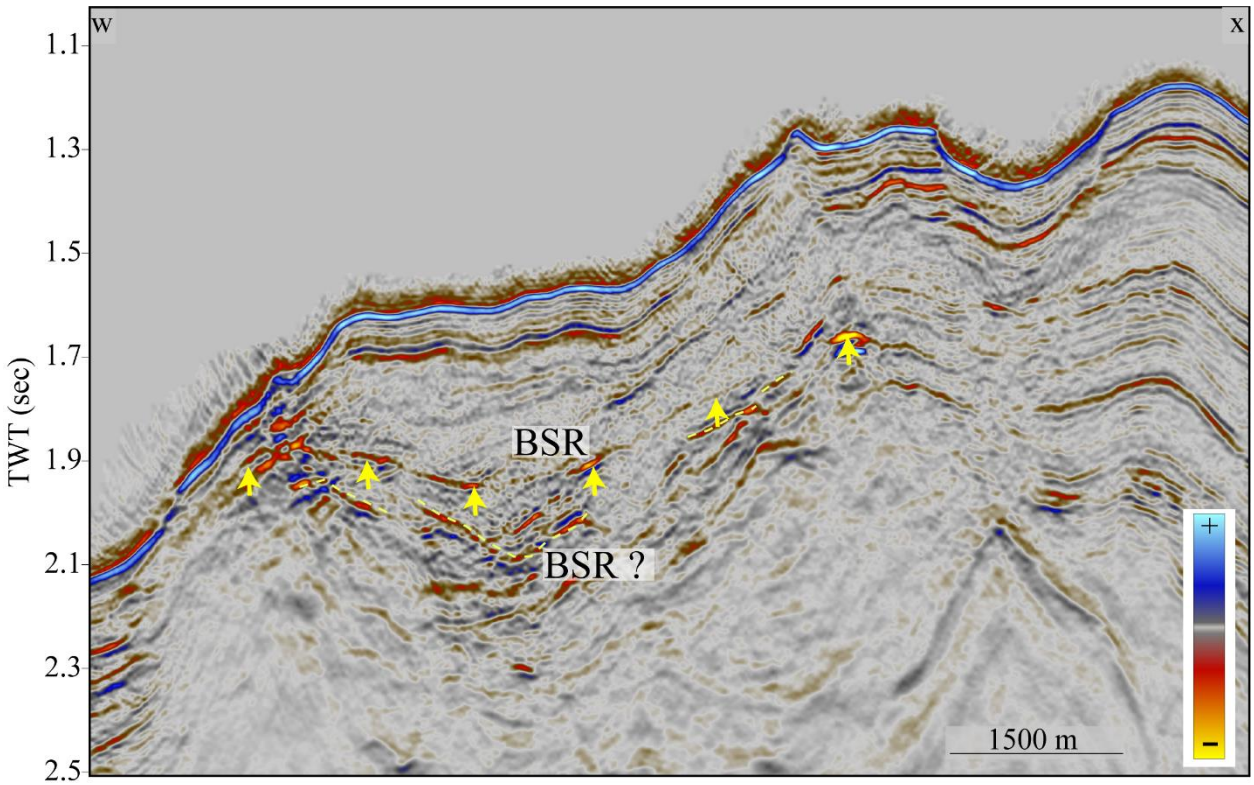

Figure 24: A seismic profile showing a south-north cross-section across the northern BSR system of Zone-3. A discontinuous BSR is marked with yellow arrows. A potential second BSR is marked with yellow dashed line. The profile location is shown in Figure 21.

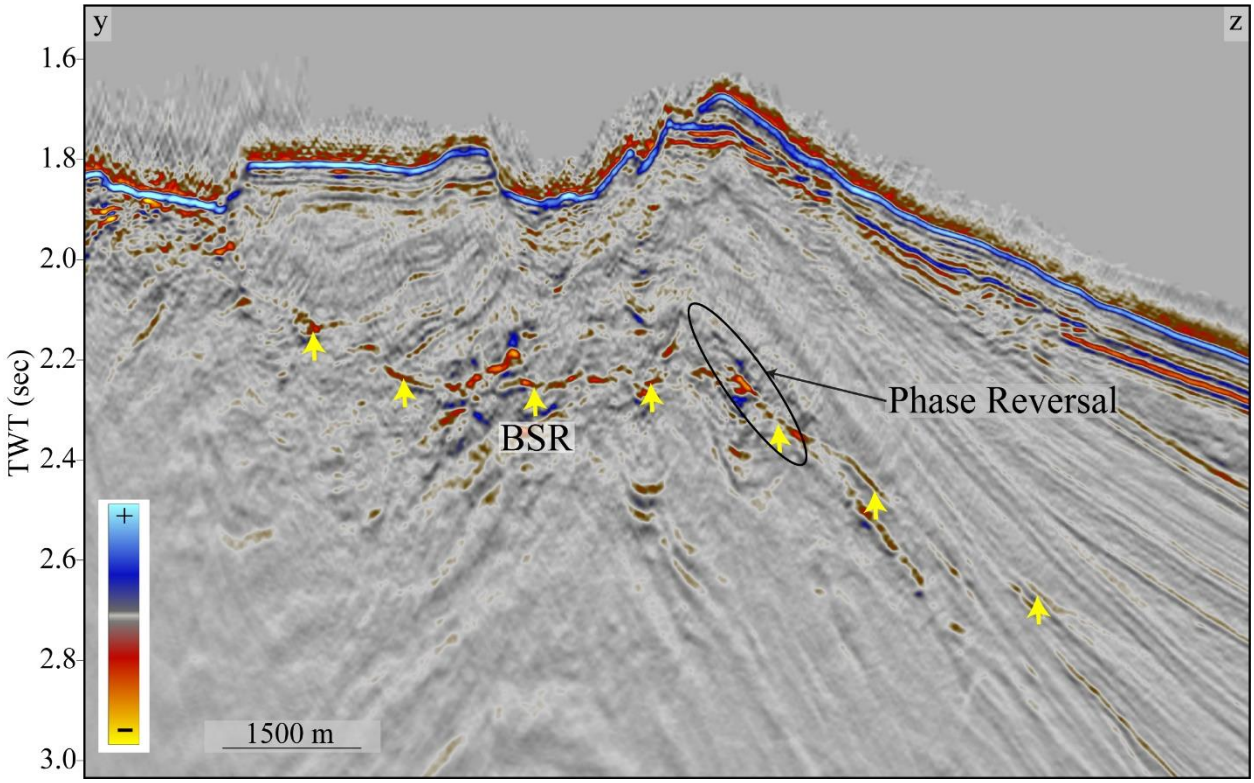

Figure 25: A seismic profile showing a north-south cross-section across the southern BSR system of Zone-3. A discontinuous BSR is marked with yellow arrows. The profile location is shown in Figure 21.

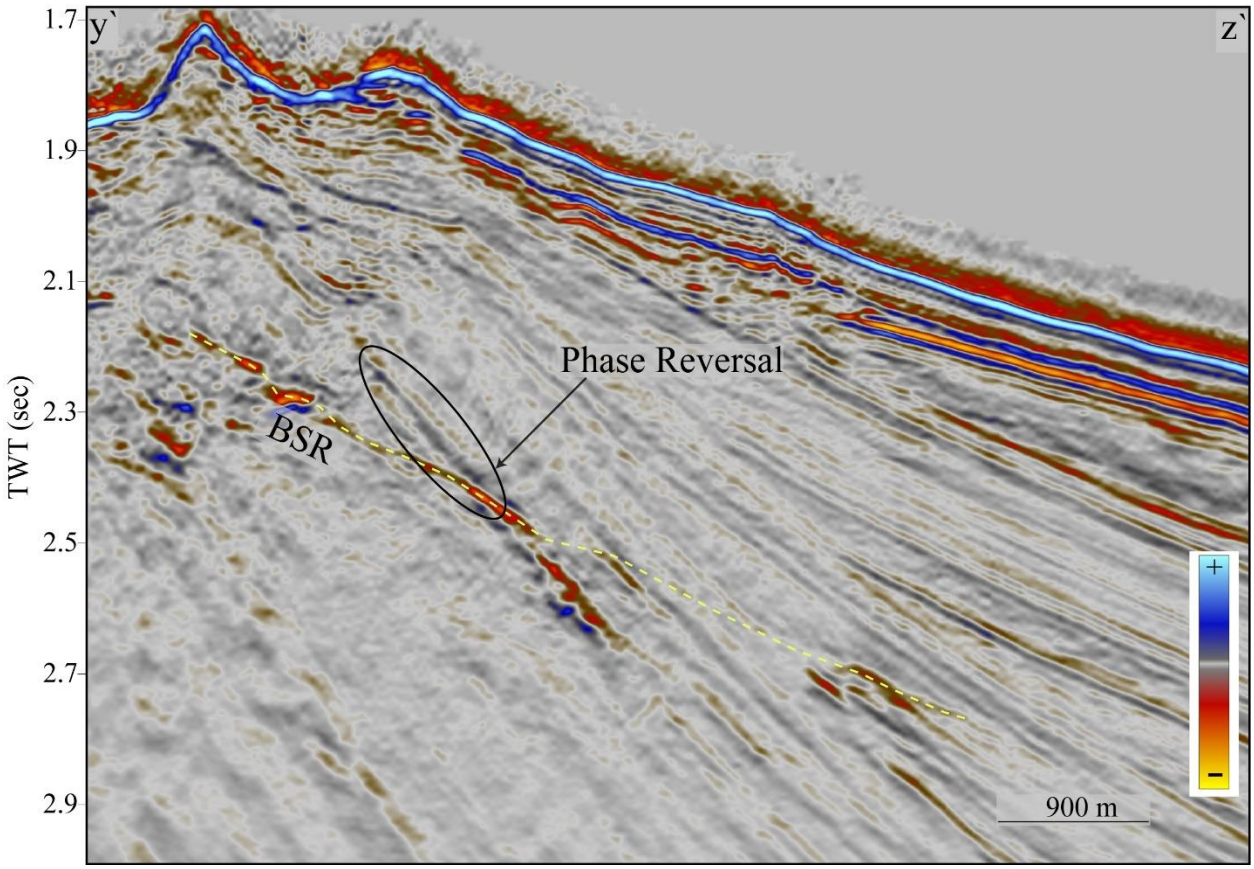

Figure 26: A seismic profile showing a north-south cross-section across the southern BSR system of Zone-3. A discontinuous BSR is marked with yellow line. The profile location is shown in Figure 21.

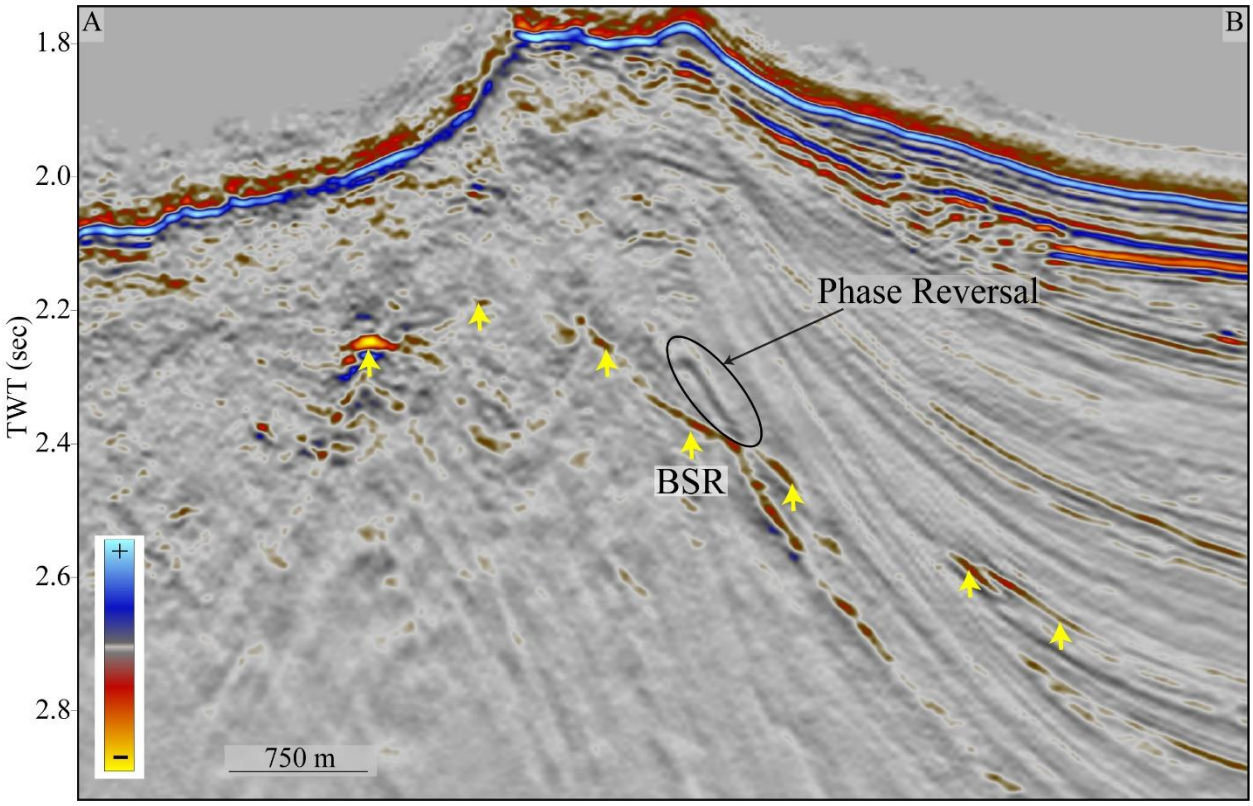

Figure 27: A seismic profile showing a west-east cross-section across the southern BSR system of Zone-3. A discontinuous BSR is marked with yellow arrows. The seismic phase reversal associated with the different acoustic properties of free gas vs. gas hydrate is noted on the figure. The profile location is shown in Figure 21.

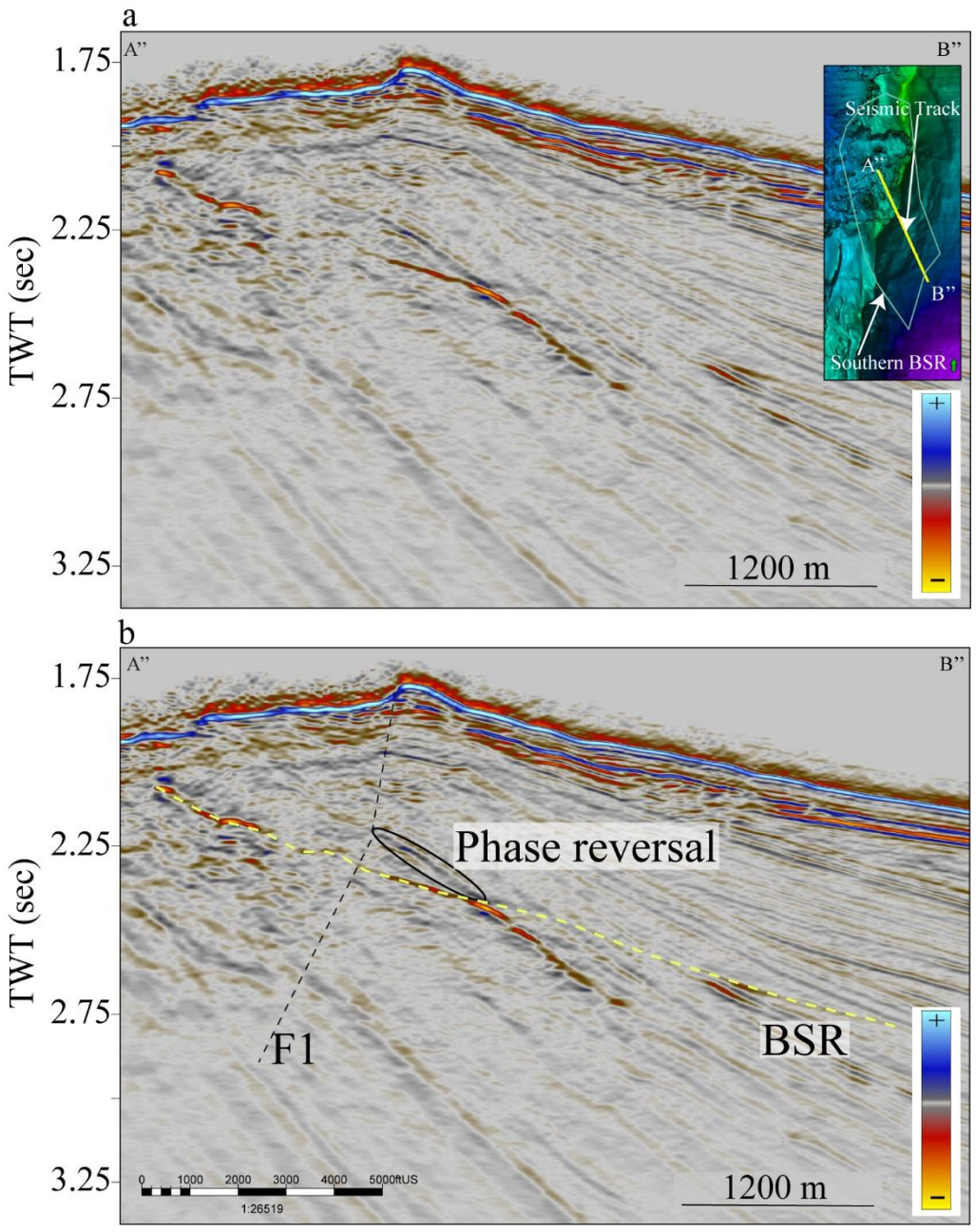

Figure 28: a) An uninterpreted seismic profile across the southern BSR showing the arbitrary cross-section. b) Interpreted cross-section of the seismic profile shown in a).

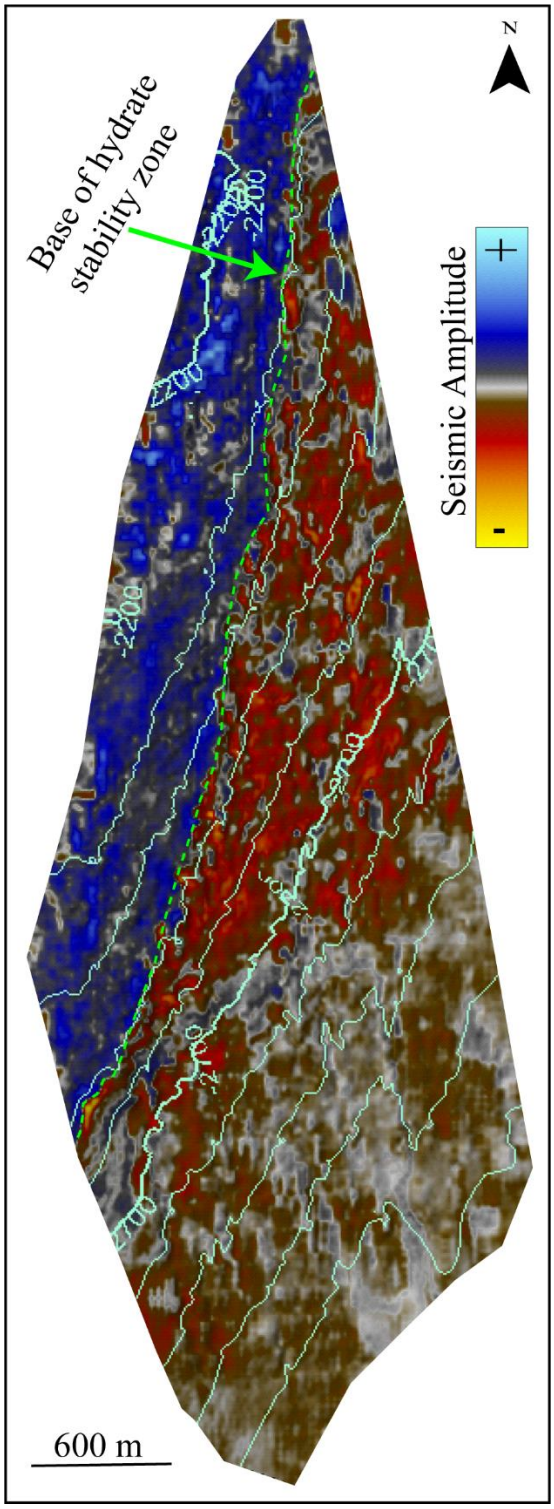

Figure 29: Instantaneous amplitude map along the reflector showing the phase reversal in the southern BSR system in Zone-3 (Figures 23-25). Here, blue color indicates the extent of peak-leading reflections that may be associated with the presence of hydrates. Contours represent TWT (msec) times of the reflector. The location of peak-leading reflection is shown in Figure 21.

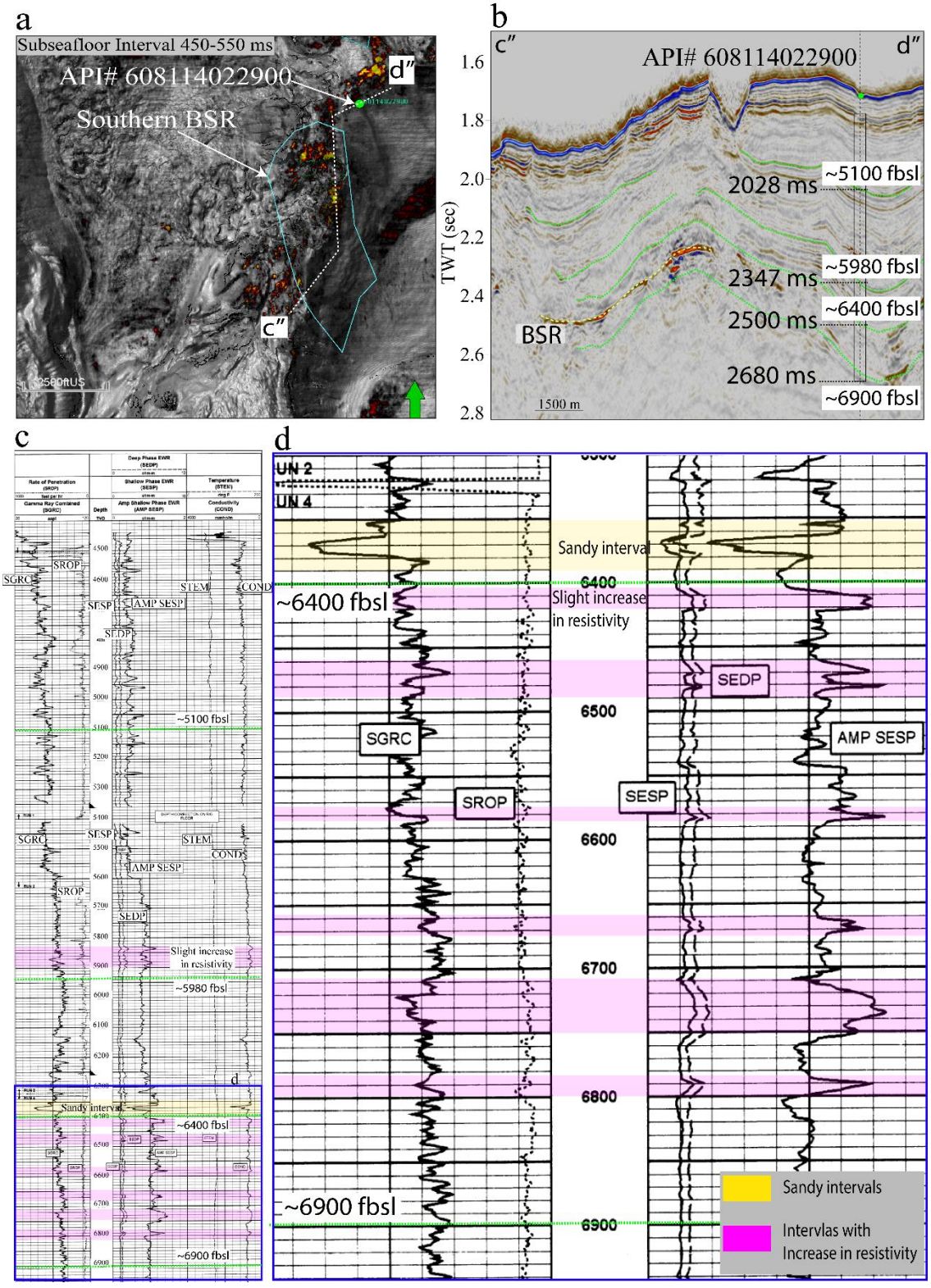

Figure 30: a) The map shows the RMS amplitude in the proximity of the southern BSR of Zone-3 within the subsurface interval of 450-550 ms. The green circle shows the location of the well with

API# 608114022900, and the white dotted line is the track of the seismic profile shown in b). c) The well logs are shown in Figure c). A Zoom-in section of the logs at a depth interval of ~6300-6950 ft is shown in Figure d. Scales: SROP (1000-0), SGRC (20-120), SEDP (1-10), SESP (1-10), AMP SESP (1-2), STEM (0-200), COND (4000-0).

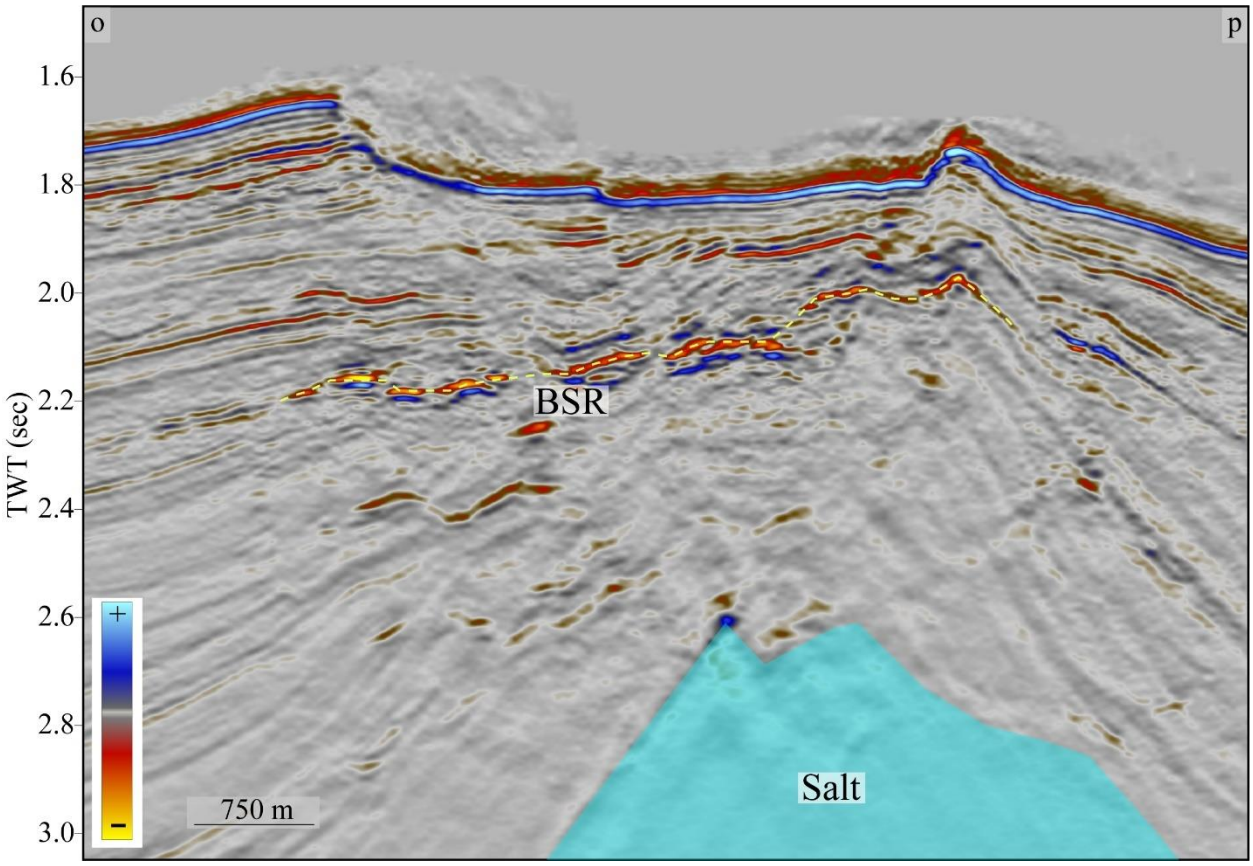

Figure 31: A seismic profile showing a west-east cross-section across the eastern BSR system of Zone-3. A discontinuous BSR is marked with dashed lines. The profile location is shown in Figure 21.

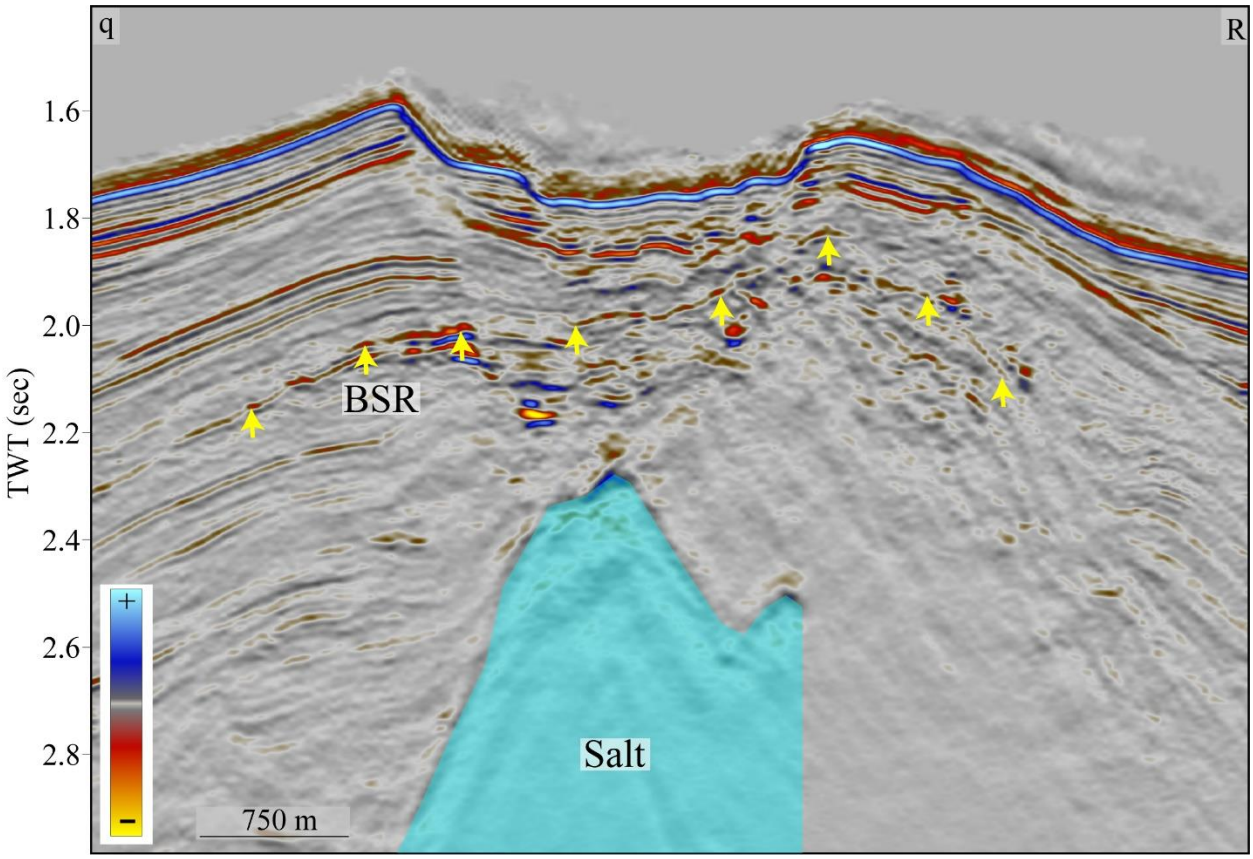

Figure 32: A seismic profile showing a west-east cross-section across the eastern BSR system of Zone-3. A discontinuous BSR is marked with yellow arrows. The profile location is shown in Figure 21.

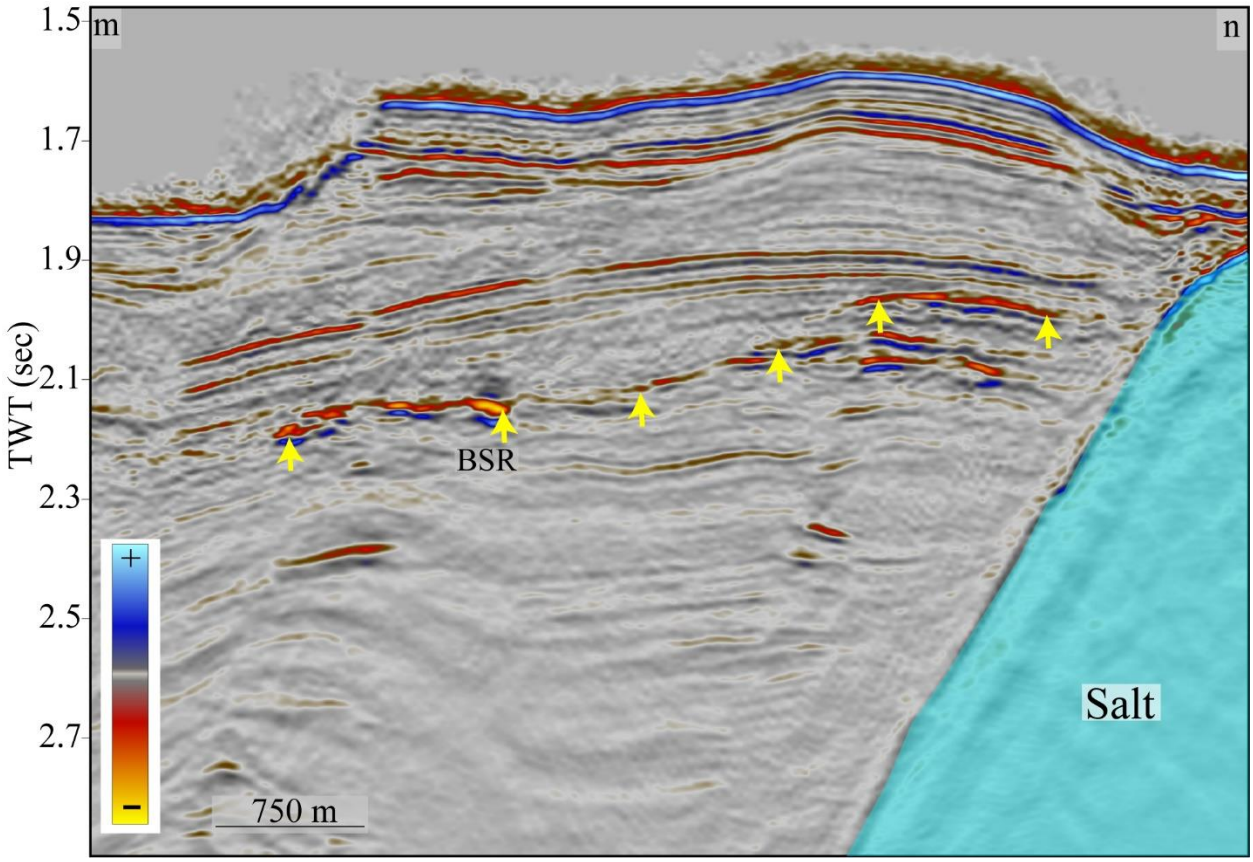

Figure 33: A seismic profile showing a north-south cross-section across the eastern BSR system of Zone-3. A discontinuous BSR is marked with yellow arrows. The profile location is shown in Figure 21.

5 Resource Estimation

We calculate high and low estimates for the high-confidence gas hydrate accumulations based on the total area of peak-leading reflections above the BSRs. The low estimate is based on a 10 m-thick sand layer, 30% porosity, and 50% gas hydrate saturation. The high estimate assumes 30 m-thick sand layer, 40% porosity and 90% gas hydrate saturation. The Project Area 2.4 report provides details about the methodology and parameters used for resource estimation in this report.

In Project Area 2.2, we map peak leading reflections in Zone-1 (Figure 14) and Zone-3 (Figure 29) that occupy a total area of 3.5 km^2. This results in minimum and maximum gas resource estimates of 0.9 and 6 billion cubic meters (BCM) or 31.8 and 211.9 billion cubic feet (bcf) respectively at STP (standard temperature and pressure).

6 Conclusions

We map six BSRs in Project Area 2.2 that span a total area of ~203 km^2. All mapped BSRs are associated with salt ridges and salt diapirs and are highly influenced by structural elements like faults, fractures, and vents. These structural elements likely act in some capacity to focus the gas to the overlying hydrate systems. Most of the BSRs in this area are discontinuous.

We mapped a peak-leading reflection in Zone-1, which only covers a very small area of ~1 km^2. Apart from this peak-leading reflection, we observe a patch of phase reversal in the southern BSR of Zone-3. This patch spans an area of ~ 2.5 km^2 and likely has hydrate present in high saturation. However, the lack of well data within many BSR systems prevents further in-depth analysis of the BSR systems identified.

Considering only the peak-leading reflection and phase reversals, we estimate the volume of free gas at STP in this area of ~0.9 – 6 BCM, 31.8 and 211.9 billion cubic feet (bcf). However, this is just a rough estimation as the presence and characterization of peak-leading reflection is strongly influenced by the data quality and signal frequency, which is not favorable for this project area.

7 References

Bureau of Ocean Energy Management, 2017, BOEM Northern Gulf of Mexico Deepwater Bathymetry Grid from 3D Seismic. Retrieved November 25, 2022, from https://www.boem.gov/oil-gas-energy/mapping-and-data/map-gallery/northern-gom-deepwater-bathymetry-grid-3d-seismic.

Carter, R. C., Gani, M. R., Roesler, T., and Sarwar, A. K. M. (2016). Submarine channel evolution linked to rising salt domes, Gulf of Mexico, USA. *Sedimentary Geology*, *342*, 237–253. https://doi.org/10.1016/j.sedgeo.2016.06.021

Hillman, J. I. T., Cook, A. E., Sawyer, D. E., Küçük, H. M., and Goldberg, D. S. (2017). The character and amplitude of 'discontinuous' bottom-simulating reflections in marine seismic data. *Earth and Planetary Science Letters*, *459*, 157–169. https://doi.org/10.1016/j.epsl.2016.10.058

McConnell, D. R., and Kendall, B. A. (2002). Images of the Base of Gas Hydrate Stability, Northwest Walker Ridge, Gulf of Mexico. *Proceedings of the Annual Offshore Technology Conference*, 1009–1018. https://doi.org/10.4043/14103-ms

Portnov, A., Cook, A. E., Sawyer, D. E., Yang, C., Hillman, J. I. T., and Waite, W. F. (2019). Clustered BSRs: Evidence for gas hydrate-bearing turbidite complexes in folded regions, example from the Perdido Fold Belt, northern Gulf of Mexico. *Earth and Planetary Science Letters*, *528*, 115843. https://doi.org/10.1016/j.epsl.2019.115843

Sassen, R., Losh, S. L., Cathles, L., Roberts, H. H., Whelan, J. K., Milkov, A. V., et al. (2001). Massive vein-filling gas hydrate: Relation to ongoing gas migration from the deep subsurface in the Gulf of Mexico. *Marine and Petroleum Geology*, *18*(5), 551–560. https://doi.org/10.1016/S0264-8172(01)00014-9

Shedd, W., Boswell, R., Frye, M., Godfriaux, P., and Kramer, K. (2012). Occurrence and nature of " bottom simulating reflectors" in the northern Gulf of Mexico. *Marine and Petroleum Geology*, *34*(1), 31–40. https://doi.org/10.1016/j.marpetgeo.2011.08.005

Triezenberg, P. J., Hart, P. E., and Childs, J. R. C. (2016). National Archive of Marine Seismic Surveys (NAMSS): A USGS data website of marine seismic reflection data within the US Exclusive Economic Zone (EEZ).". *US Geological Survey Data Release 10*, *F7930R7P*.

Vanneste, M., De Batist, M., Golmshtok, A., Kremlev, A., and Versteeg, W. (2001). Multi-frequency seismic study of gas hydrate-bearing sediments in Lake Baikal, Siberia. *Marine Geology*, *172*(1–2), 1–21. https://doi.org/10.1016/S0025-3227(00)00117-1